Structural-topological preferences and protonation sequence of aliphatic polyamines: a theoretical case study of tetramine *trien*

Adedapo S. Adeyinka and Ignacy Cukrowski*

Department of Chemistry, Faculty of Natural and Agricultural Sciences, University of Pretoria, Lynnwood Road, Hatfield, 0002 Pretoria. South Africa

*Corresponding author:
ignacy.cukrowski@up.ac.za
Landline: +27 12 420 3988
Fax: +27 12 420 4687

Keywords: linear polyamines, trien, structural preferences, topological preferences, protonation sequence, DFT

Abstract

A large set of lowest and medium energy conformers of aliphatic tetramine *trien* was used to uncover structural-topological preferences of poliamines. Numerous common structural features among **HL** and **H_2L** tautomers were identified, *e.g.*, H-atoms of protonated functional groups are always involved in intramolecular NH•••N interactions and they result in as large and as many as possible rings in lowest energy conformers. Largest, 11-membered, rings stabilize a molecule most and they appeared to be strain free whereas 5-memebred-rings were most strained (all formed due to NH•••N interactions). The CH•••HC interactions with QTAIM-defined atomic interaction lines were also found but, surprisingly, mainly in the lowest energy conformers of **HL** tautomers. According to the Non-covalent Interaction-based (NCI) analysis, 5-memebered rings formed by CH•••HC interactions are not strained and, in general, 3D NCI isosurfaces mimic those obtained for weaker NH•••N interactions. Also, 3D NCI isosurfaces found for NH•••N and CH•••HC interactions, regardless whether linked or not by an atomic interaction line, appeared to be indistinguishable. Using lowest energy conformers, theoretically predicted mixture of primary (**HL_p**) and secondary (**HL_s**) forms of *trien* was found to be in accord with the literature reports; using linear conformers resulted in predicting **HL_s** as the only tautomer formed. In contrast to HF, the overall performance of B3LYP was found satisfactory for the purpose of the study; it reproduced MP2 results well.

Keywords: linear aliphatic polyamines; protonation sequence; trien; QTAIM, NCI, DFT.

1. Introduction

Some 'families' of organic compounds, even though they might play significant roles in many fields of chemistry or biochemistry, have not been extensively explored computationally at higher than MM-levels of theory. In many cases, this can be attributed to an almost 'infinite' number of possible conformations that higher homologues can adopt due to their enormous flexibility making this kind of investigation an extremely challenging task. A typical example might be linear aliphatic polyamines (LAPs) which are found in most living organisms and are important in the regulation of cell proliferation and cell differentiation [1-3]. Their function in living organisms is based on their ability to act as natural polycations when protonated under physiological conditions and therefore interact with natural polyanions such as DNA and RNA thereby influencing important cell functions [3]. Due to their crucial roles, among others in physiological processes, the protonation sequence of LAPs has been investigated with various experimental techniques for decades but a consensus has not been reached as to which of the nitrogen atoms present in a given polyamine is protonated in the first step [4-12]. For instance, Paoletti et al. suggested, from thermochemical studies of diethylenetriamine (*dien* or 2,2-tri) and triethylenetetramine (*trien* or 2,2,2-tet), that the first step of protonation results in the formation of an equilibrium mixture of tautomers with either the primary ($\mathbf{HL_p}$) or secondary ($\mathbf{HL_s}$) nitrogen atoms protonated [4]. Hague and Moreton, on the other hand, concluded from ^{13}C NMR studies of a wide spectrum of polyamines, ranging from 2,2-tri to tetraethylenepentamine (2,2,2,2-pent), that all the nitrogen atoms in the monoprotonated form share the proton equally [5]. Contrary to these, Delfini et al [7] proposed from ^{13}C NMR study of a series of triamines that (i) in the case of symmetrical triamines, either of the identical primary N-atoms is involved in the first protonation step for symmetrical molecules, but (ii) for asymmetrical triamines, the primary nitrogen atom attached to the longer aliphatic chain is protonated first. Recently, Borkovec et al [8] used cluster expansion analysis on experimental NMR data to investigate a number of di-, tri-, tet- and pentamines. They concluded that both forms, $\mathbf{HL_p}$ and $\mathbf{HL_s}$, are formed in the first protonation step but $\mathbf{HL_p}$ is predominant with a %-fraction of 86%. Clearly, even in some cases, where the same experimental technique was used, such as ^{13}C NMR, different research groups proposed contradicting conclusions [8, 9].

Conformational preference of LAPs with more than two nitrogen atoms has not been investigated computationally. However, better understanding of the properties of polyamines and their activity, as observed from experimental investigations, requires knowledge of their conformational preferences [13]. Furthermore, if one could theoretically predict a reliable and representative set of the lowest energy conformers (LECs) of all protonated forms of polyamines then this, *e.g.*, (i) should be of great aid in interpretation of experimentally recorded NMR

spectra (often used to predict most likely protonation sequence) or (ii) might result in significantly improved quality of theoretically computed protonation constants, as it has been demonstrated in the case of carboxylic acids [14,15].

Therefore, we have embarked on the development and testing of a dedicated protocol for conformational analysis of mono- and di-protonated (**HL** and **H_2L**) forms of LAPs and, as a case study, results obtained for triethylenetetramine (*trien*) are reported in this work. The singly protonated form of *trien* is of particular interest to us mainly because (i) there is no consensus in the literature as to the preferred site of protonation and (ii) in the case of symmetrical LAPs, such as *trien*, the basicity of the primary and secondary N-atoms is of the same order of magnitude [7,16]. Furthermore, the apparent difficulty in characterizing the singly protonated forms of LAPs by, *e.g.*, XRD crystallography, has been a major hindrance; we were able to find only one example of the singly protonated LAP, namely that of 2,2-tri reported by Ilioudis et al [17]. We were also motivated by the fact that, except for few alicyclic diamines which were mainly studied using molecular mechanics, MM, methods [14, 19-20] the conformational analysis of these important compounds, as far as we could establish, has not been reported to date. Both Raman spectroscopy and MM-based theoretical results [18-20], however, led to the conclusion that the most stable conformers are those in which either intra- or intermolecular interactions can occur depending on whether the isolated diamine was studied in the solid or aqueous phase. Also the results showed that even though the conformational barriers obtained with MM method compare very well to those from *ab initio* results for cyclic polyamines, this is not always the case for aliphatic polyamines [19, 20].

Hence, in this work apart from characterizing the lowest energy conformers of mono and di-protonated *trien*, we have also embarked on a study of their conformational preferences in terms of structural and topological properties. Unavoidably, this kind of study is computationally expensive because it involves modelling of hundreds (if not thousands) of conformers. With an attempt to suggest most economical methodology, we have also evaluated, relative to MP2, performance of HF and selected, B3LYP and B97D, DFT techniques.

2. Methodology

2.1 Computational details

Energy minimized structures and wavefunctions were generated from Gaussian 09, Revision B [21] at the HF, B3LYP, B97D and MP2 theory levels in solvent using the polarizable continuum model [22-24] in conjunction with the UFF cavity model with water as a solvent (ε = 78.39). Unless otherwise stated, the 6-311++G(d,p) basis set was used; it has been shown that this basis set contains adequate polarization and diffuse functions sufficient to describe molecules like

polyamines [25,26]. General shortcomings as well as advantages of each levels of theory tested here are well-known. However, due to a formidable computational task associated with the aim of this work, it was important to find out which level of theory is best suited for the purpose. In other words, which level of theory performs sufficiently well to identify the lowest energy conformers and characterize their structural preferences without getting involved in unnecessarily time-consuming computational operations.

The Quantum Theory of Atoms in Molecules (QTAIM) [27], as implemented in AIMAll [28] together with the recently developed non-covalent interaction (NCI) index technique [29], were used to carry out a topological analysis of the calculated electron densities in order to identify and characterize intramolecular interactions which may be responsible for conformational preference. All topological data (QTAIM and NCI) as well as molecular graphs and NCI 3D plots were generated with AIMAll. Frequency calculations were performed on fully optimized geometries to ensure that the true stationary points were found; in case of MP2, the frozen core approximation was used. No imaginary frequencies were found among (i) all MP2-optimized conformers and (ii) lowest energy conformers at all levels of theory. Few conformers of diprotonated form of *trien* with a single imaginary frequency are listed in Table S1 in the Supplementary Information (SI). The conformational search was done using MM force field (MMFFaq) and the Monte Carlo method as implemented in the Spartan [30] quantum chemistry package.

2.2 Conformational search protocol

The potential energy surface of extremely flexible biomolecules, such as aliphatic polyamines, is characterized by the presence of an enormous number of local minima, thus making an exhaustive conformational analysis impracticable, particularly if DFT was to be employed exclusively. Hence, we decided to develop a most efficient (for the study of polyamines) conformational search protocol involving both, MM and *ab initio* techniques. One of our major goals was to identify a 'final' subset of LECs containing representative structures within a narrow (few kcal/mol, typically within 5 kcal/mol) relative energy range, $\Delta E = E_{\mathrm{conf}} - E_{\mathrm{LEC}}$ (E_{conf} stands for the electronic energy of a conformer). We used ΔE rather than ΔG values because (i) the latter requires frequency calculations, an additional and extremely time consuming operation we wanted to avoid (if possible), (ii) this work is not concerned with protonation constants calculations (this would require ΔG values) and (iii) we needed representative sets of polyamines at minimum computational time and, fortunately, under conditions employed the relative trends in the ΔE and ΔG values did not differ significantly enough to justify the use of ΔG values as a selection criterion.

The capped-stick representations (with numbering of atoms) of linear structures of only two possible **HL$_p$** (primary N-atom is protonated) and **HL$_s$** (secondary N-atom is protonated) tautomers used as inputs for conformational search by MM are shown in Fig. 1(a and b). Hypothetically, there are four possible tautomers of the di-protonated form, but only two of them, **H$_2$L$_{ps}$** (with primary and secondary N-atom protonated) and **H$_2$L$_{pp}$** (with both primary N-atoms protonated) were considered in this work, see Fig. 1(c and d), based on minimum charge separation constraints required by electrostatics.

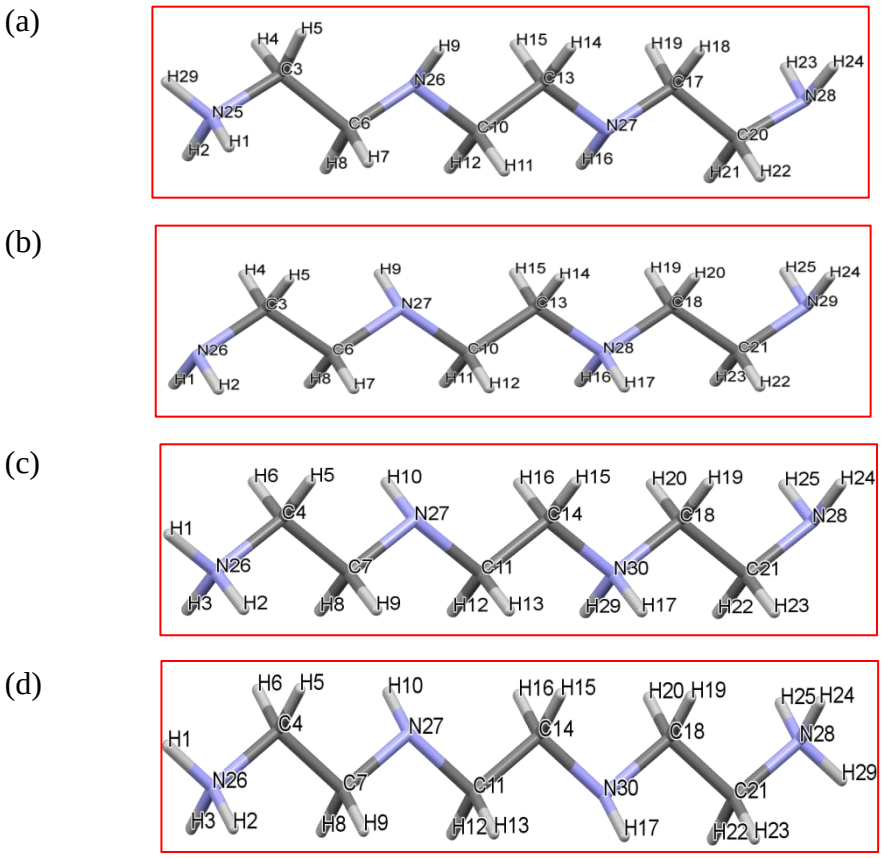

Fig. 1 Capped-stick representation of linear structures of the mono-protonated: (a) - HL$_p$ and (b) - HL$_s$, and di-protonated: (c) – H$_2$L$_{ps}$ and (d) – H$_2$L$_{pp}$, tautomers of *trien* used as inputs for conformational search by MM, also showing atoms' numbering

Each tautomer has nine single bond (N–C and C–C) torsional degrees of freedom. For each rotatable bond, a systematic variation in six steps of 60° was allowed in conformational searches. Due to the enormous number of possible conformers generated from MM-based search (*e.g.*, there are over 10 million theoretically predicted by Spartan possible conformers for each of the **HL** tautomers) one is immediately faced with a challenge, namely (i) how many to retain and (ii) how large a MM-energy window must be used within which retained conformers should fall.

Furthermore, it is important to stress that in this study we needed not only LECs but also representative structures of medium and higher energy conformers necessary to investigate their structural preferences and topological characteristics. To achieve our goals we decided to

implement a multi-stage approach which would allow us to eliminate, after each stage, the 'redundant' structures when aims of this work are concerned - see self-explanatory Scheme 1 and detailed description of each stage in PART 1 in the SI.

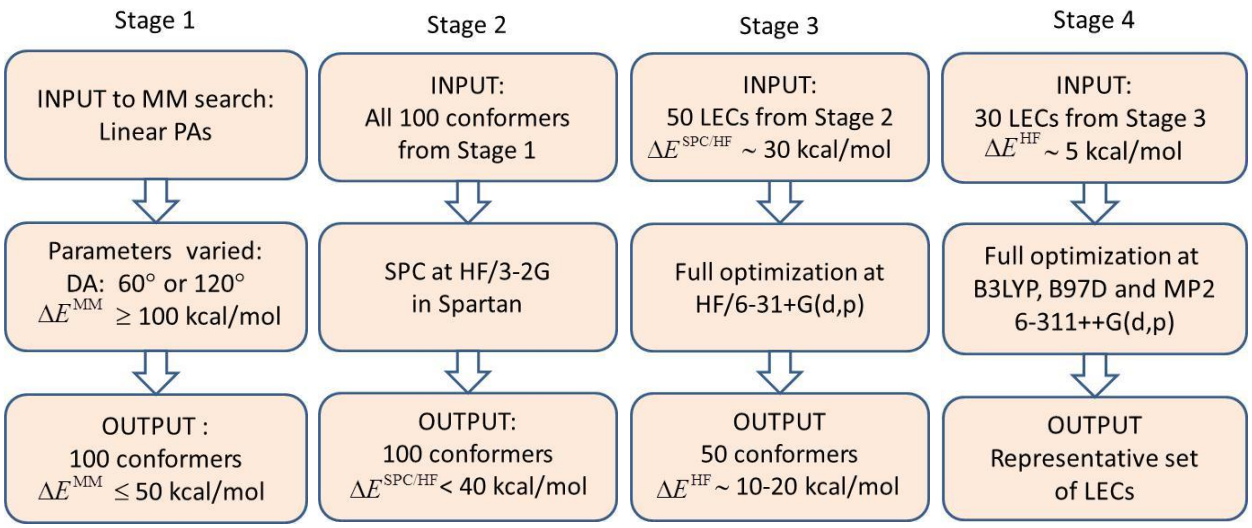

Scheme 1 Four-stage protocol implemented in the search of representative lowest energy conformers

3. Results and discussion

The structural and topological data generated at lower than MP2 level of theory are presented as differences rather than absolute values. As an example, when interatomic distances d(H,N) for the intramolecular NH•••N interactions are analysed, we will report data obtained at, *e.g.*, HF, as $\Delta d(H,N)_{HF} = d(H,N)_{HF} - d(H,N)_{MP2}$. Using this approach made it easier to evaluate the relative performance of a lower level of theory. Moreover, one must remember that performing all the calculations at the MP2 level on a large number of conformers is extremely time-consuming and, importantly, not always necessary to achieve goals of interest. To facilitate data analysis and to monitor the performance of the conformational search implemented here, we have consistently labelled conformers of the primary (**HL_p**) and secondary (**HL_s**) forms of monoprotonated *trien* as C_pn and C_sn, respectively. Those of the di-protonated forms, **H_2L_{ps}** and **H_2L_{pp}**, have been labelled as $C_{ps}n$ and $C_{pp}n$, respectively, where $C_{ps}n$ is used for conformers of the tautomeric form where one primary and one secondary nitrogen atoms are protonated whereas $C_{pp}n$ is used to denote a structure in which the two terminal nitrogen atoms are protonated. For all tautomers *n* stands for the identification number of a conformer as obtained from the MM-based conformational search where $n = 1$ applies to the lowest MM-energy conformer.

3.1 Analysis of conformers' relative energies

The full data sets of $\mathbf{HL_p}$, $\mathbf{HL_s}$, $\mathbf{H_2L_{ps}}$ and $\mathbf{H_2L_{pp}}$ conformers optimized at **Stage 4** of the conformational protocol are included in Table S2 of the SI and relevant bar-graphs are shown in Fig. S1 of the SI. For illustration purposes, relative energies and Boltzmann distribution, as %-fraction of the total population of conformers considered, of ten LECs of $\mathbf{HL_p}$ conformers of *trien*, obtained from **Stage 4** at different levels of theory are shown in Fig. 2.

Let us first focus on the MP2-generated data from which it is apparent that:

- According to the Boltzmann distribution, there are only few (between 3 and 5) conformers of each tautomer that contribute significantly (>5%) to their populations.
- There are always one or two conformers which are significantly lower in energy when compared with the remaining LECs. Importantly, we found that these two conformer are always among the top 12 conformers generated from MM search; among the lowest energy conformers, the largest $n = 12$ was found for the di-protonated $\mathbf{H_2L_{pp}}$ form.
- It appears that top 25 MM-generated conformers (of the lowest energy) 'guaranty' fully representative set of MP2-optimized structures, each one contributing to the total population 3% and above. If $C_{ps}41$ is excluded (note that the energy of this conformer is essentially the same as that of $C_{ps}10$; this exemplifies the need of optimizing small sets of DFT-generated LECs at the MP2 level) then the $C_{pp}23$ has the largest $n = 23$ value.
- The energy window of 30 conformers (output from **Stage 4** in Scheme 1) decreases from $\mathbf{HL_p}$ to $\mathbf{H_2L_{pp}}$ (from 15 to 5.6 kcal/mol, respectively); the larger number of conformers of similar energy is observed for the $\mathbf{H_2L_{pp}}$ form of *trien* and this is due to specific structural features of this tautomer, as discussed in the following section.

The above analysis strongly suggests that the protocol implemented here has indeed provided us with (i) representative sets of the lowest energy conformers (recall that we have fully optimized 30 top MM-generated conformers at all levels of theory) as well as (ii) sufficient spread in conformers' energies (see Table S2 of the SI) needed to explore conformational preferences in terms of structural and topological properties. Furthermore, data presented in Table 2 of the SI also shows that:

- Without an exemption, the top MP2 conformer of all tautomers is also reproduced as the lowest energy at the B3LYP level.
- Top four MP2 conformers of $\mathbf{HL_p}$, $\mathbf{HL_s}$ and $\mathbf{H_2L_{ps}}$ are also among top four at B3LYP and B97D whereas top five MP2 conformers of $\mathbf{H_2L_{pp}}$ (they contribute above ~5% to the total population) are among top 10 conformers at the B3LYP level (they contribute above ~3%

to the total population) when conformers with one imaginary frequency, $C_{pp}01$ and $C_{pp}04$, are excluded.

- Grouping of conformers in terms of their relative energies is similar at the DFT and MP2 levels. It means that if just few lowest energy conformers are observed at DFT then these conformers will be even more dominant, as LECs, at MP2. It also appears that if a large number of similar in energy conformers is generated at the DFT level, the same is also obtained at MP2 although each time MP2 differentiates the relative energies better.
- If only the lowest energy conformers are required then it is sufficient to select those from the B3LYP optimization which contribute above ~3% to the total population and subject them to optimization at MP2.

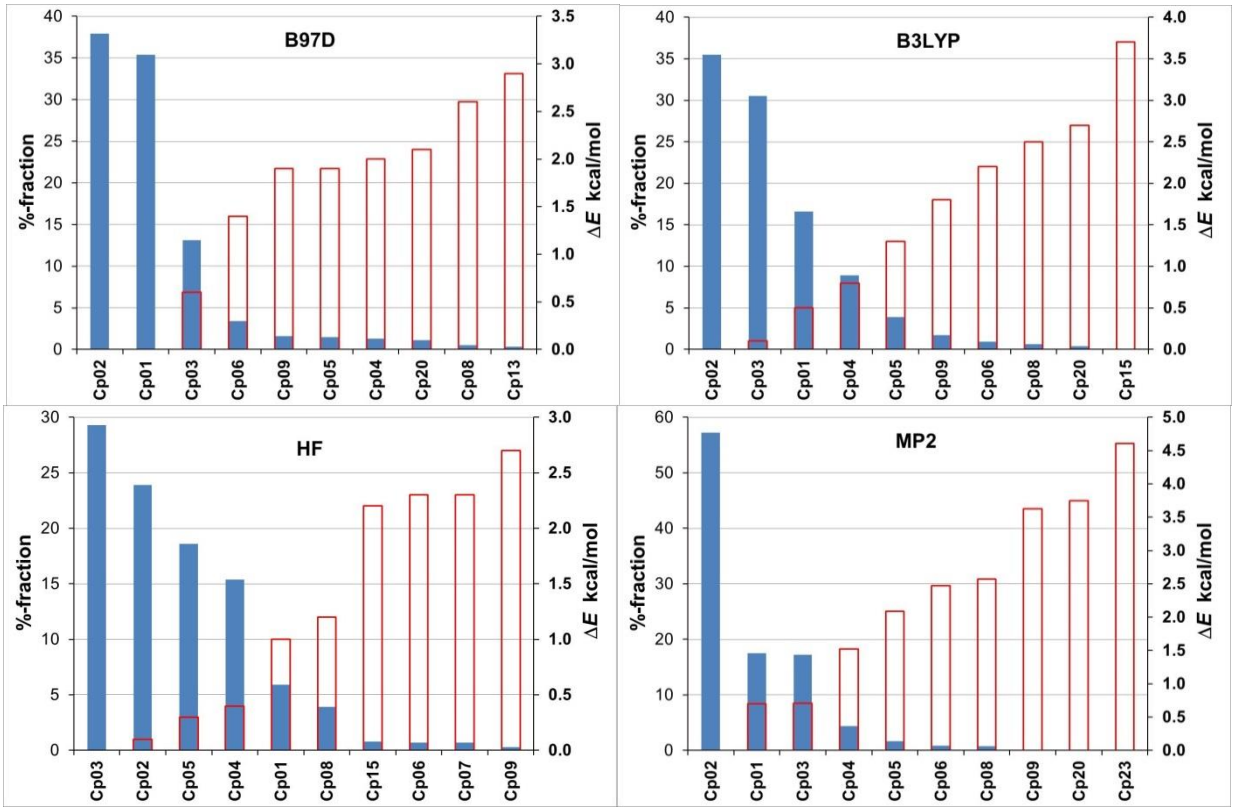

Fig. 2 Graphical presentation of ten lowest energy HL_p conformers of *trien*, in terms of %-fraction computed from Boltzmann distribution (solid bars) and relative energies (in kcal/mol) obtained at the indicated level of theory

We have also performed an additional and extensive computational modelling (for details see PART 2 of the SI) which fully confirmed that the implemented search protocol has been able to recover representative (i) samples of conformers needed for analyses of factors influencing conformational preferences and (ii) sets of top lowest energy conformers of each tautomer with a high likelihood that the true LEC was also found.

In general, analysis of the relative energies indicates that, as observed for other structurally flexible compounds, such as amino acids [25], the Hartree-Fock method, irrespective of basis set used, is only, if at all, useful for pre-optimization of conformers generated from the MM-search. In addition, energy differences between conformers are the smallest at HF making it difficult to decide on which ones should be retained for further analysis.

3.2 Structural preferences

Full sets of 30 structures for **HL_p**, **HL_s**, **H_2L_{ps}** and **H_2L_{pp}** are shown in Figs. S2-S5 in the SI. For convenience, the structure of the LEC and a representative sample of conformers from medium and higher energy spectrum of all tautomers obtained at MP2 are displayed in Figs. 3 and 4. An examination of all the conformers of both tautomers shows some interesting general structural features and trends (we must stress that similar geometrical features, in relation to *E*, are observed at all levels of theory examined in this work) and we will describe them separately for each tautomer of both protonated forms of *trien*.

*The **HL_p** conformers*:

a) Two H-atoms of the $–NH_3^+$ group in the LECs are involved in the formation of the NH--N short contacts. One H-atom is forming the leading 11-membered molecular ring (11m-MR) and the other forms two additional intramolecular NH--N short contacts; as a result, all N-atoms are involved in the intramolecular interactions and the largest possible number of rings is formed (11m-MR, one 7m-intramolecular ring, 7m-IR, and two 5m-IRs).
b) Among LECs which form the 11m-MR, those with the lowest energy (C_p02, C_p01, C_p03 and C_p04; they constitute over 90 % of the population) form the shortest contacts between terminal $–NH_3^+$ and $–NH_2$ groups with d(H,N) ~1.745±0.05 Å.
c) The somewhat higher energy conformers (they are characterized by either 11m-MR or largest possible intramolecular ring) have the shortest contact which involves either the terminal $–NH_3^+$ group or the secondary N-atom, *e.g.*, C_p05, C_p06, C_p07 and C_p08 where we observe d(H,N)~1.695±0.02 Å.
d) Medium energy **HL_p** conformers are characterized by the presence of an 8m-IR, due to the NH--N short contact between the $–NH_3^+$ terminal group and the farther secondary N-atom, leaving the $–CH_2CH_2NH_2$ fragment free to rotate and bent.
e) The highest energy conformers form the smallest possible 5m-IR, typically between the terminal $–NH_3^+$ and an adjacent –NH– group.

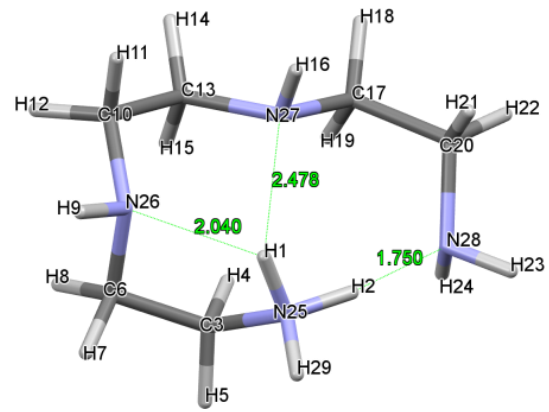

C_p02

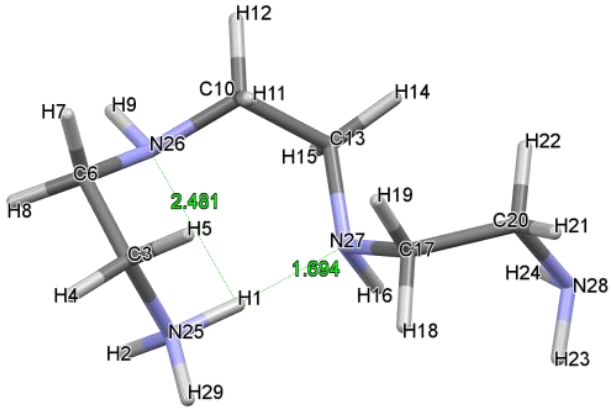

C_p29

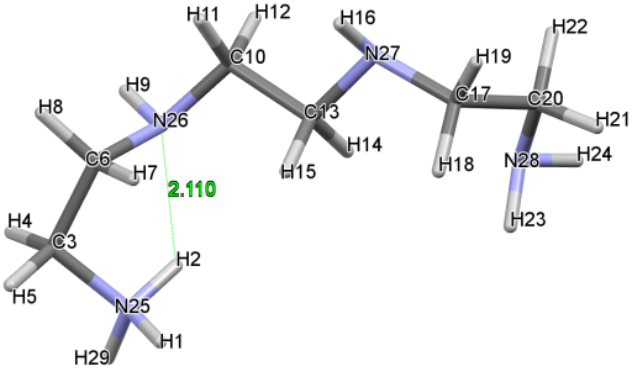

C_p43

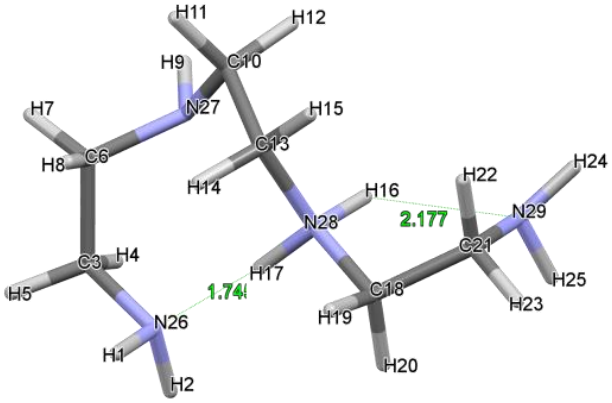

C_s04

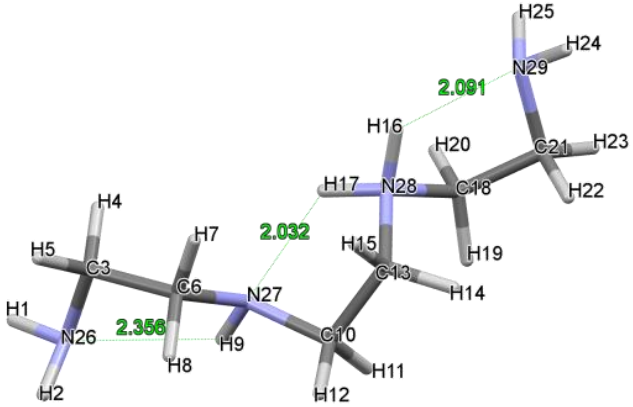

C_s07

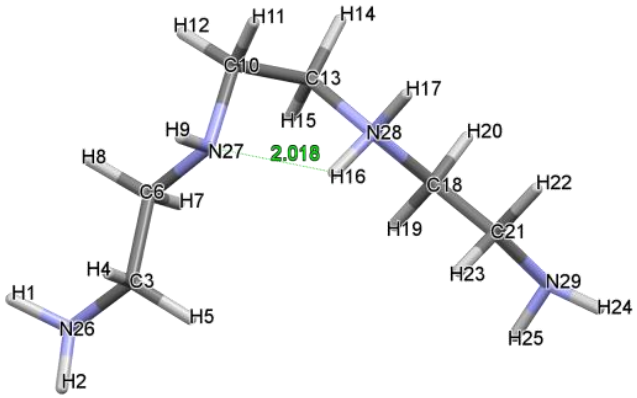

C_s41

Fig. 3 Representative structures of the lowest (C_p02 and C_s04), medium (C_p29 and C_s07) and higher (C_p43 and C_s41) energy conformers of HL_p and HL_s, respectively, generated at MP2 during the fourth and final stage of the conformational protocol developed in this work, also showing atoms' numbering as well as interatomic distances in Å of the short NH--N contacts

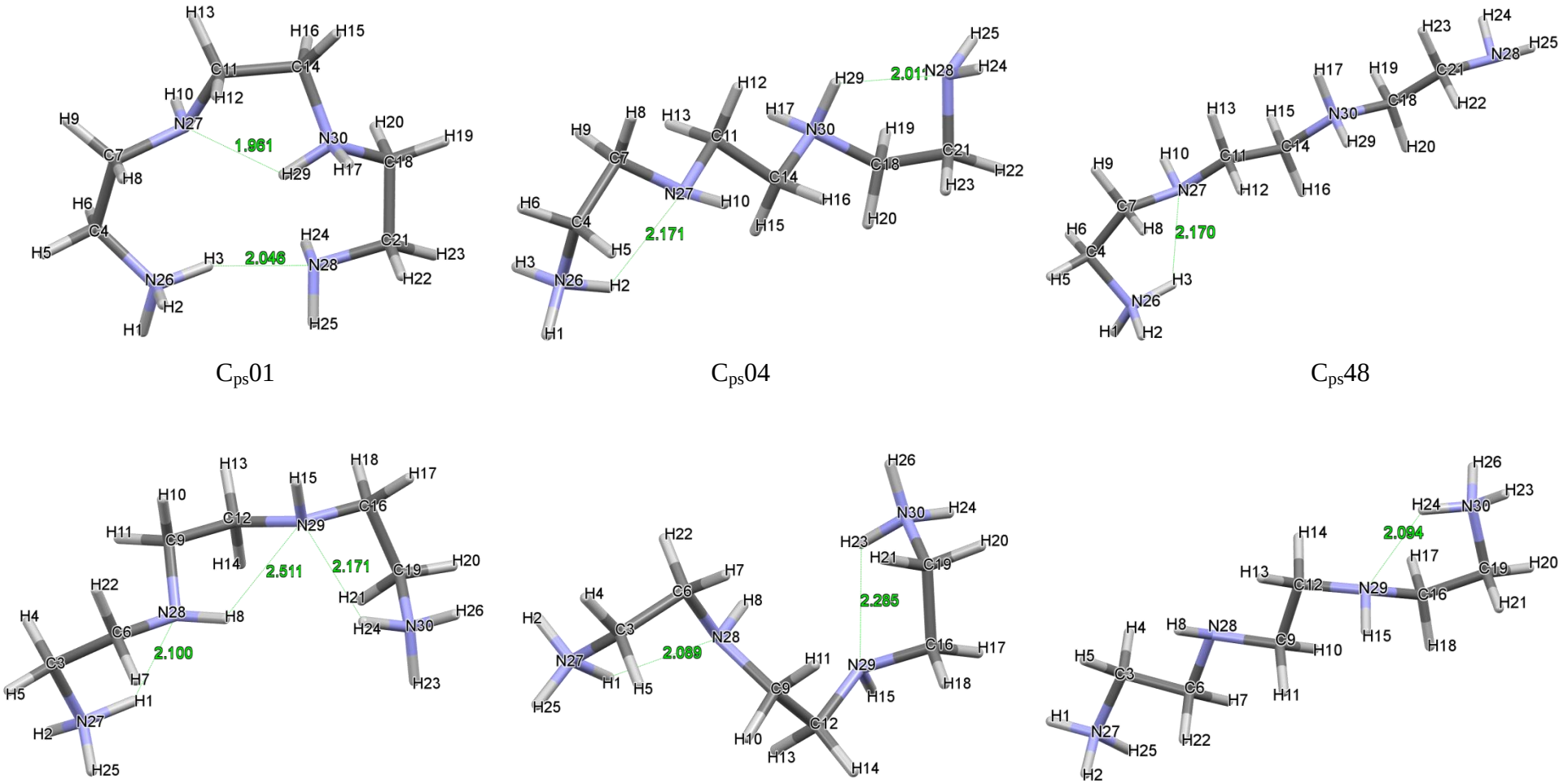

$C_{ps}01$ $C_{ps}04$ $C_{ps}48$

$C_{pp}12$ $C_{pp}27$ $C_{pp}25$

Fig. 4 Representative structures of the lowest ($C_{ps}01$ and $C_{pp}12$), medium ($C_{ps}04$ and $C_{pp}27$) and higher ($C_{ps}48$ and $C_{ps}25$) energy conformers of H_2L_{ps} and H_2L_{pp}, respectively, generated at MP2 during the fourth and final stage of the conformational protocol developed in this work, also showing atoms' numbering as well as interatomic distances in Å of the short NH--N contacts

*The **HL_s** conformers*:

a) Both H-atoms of the $–NH_2^+–$ group of the LECs are involved in the formation of the NH--N short contacts. The shortest contact with d(H,N)~1.735±0.01 Å (this generates the 8m-IR) is formed with the terminal N-atom. The other NH--N contacts involve two of the remaining unprotonated N-atoms. As a result, additional two 5m-IRs are formed, one with the terminal $–NH_2$ group where d(H,N)~2.197±0.01 Å and the other with the secondary N-atom where much longer intramolecular distance, d(H,N)~2.457±0.05 Å, is observed. In general, as one observes for **HL_p**, three rings are observed in the LECs except C_s04 (the lowest energy conformer) where only two intramolecular rings are present.
b) The medium and highest energy **HL_s** conformers have mainly smallest possible 5m-IRs and it appears that their consecutive placement is preferred.

*The **H_2L_{ps}** conformers*:

a) As found for **HL_p**, all lowest energy **H_2L_{ps}** (C_{ps}01, C_{ps}41 and C_{ps}10) conformers (i) form the 11m-MRs due to the NH--N contact between terminal functional groups but the average interatomic distance, d(H,N)~1.975±0.13 Å, is about 0.2 Å longer and (ii) with 11m-MR constitute almost 100% of the population.
b) Unlike found for the **HL_p** conformers, the NH--N contact forming the 11m-MR in the lowest energy C_{ps}01 conformer is not the shortest; the 5m-IR has shorter, by about 0.1 Å, the NH--N contact.
c) All three LECs form an additional intramolecular NH--N contact and this involves the H-atom from the $–NH_2^+–$ group of the protonated secondary N-atom and the adjacent –NH– group; as a result two, 10m- and 5m-IRs are formed.

*The **H_2L_{pp}** conformers*:

a) In general, a total of three (or minimum two) 5m-IRs are found in the LECs; we have not found a conformer with a larger intramolecular ring.
b) Among LECs, a H-atom from each of the terminal $–NH_3^+$ groups is always involved in an interaction with the N-atom of the adjacent –NH– group (regardless whether two or three 5m-IRs are found); this results in the formation of two terminal 5m-IRs. In case of three 5m-IRs being present, they are formed in consecutive fashion; the additional NH--N interaction involves two adjacent –NH– groups.
c) The medium and high energy conformers of **H_2L_{pp}** (as well as **H_2L_{ps}**) generally consist of structures with two 5m-IRs resulting from various NH--N interactions of different atoms depending on the energy range into which a particular conformer falls. Not surprisingly, their

highest in energy conformers have only one NH--N interaction resulting in the formation of the smallest possible 5m-IR, as we observed in the HECs of **HL_p** and **HL_s**.

To conclude this section, we would like to summarize and generalize all the above observations:

1) At least a single intramolecular NH--N short contact, with d(H,N) significantly shorter than the sum of the van der Waals radii, is observed in all conformers and it always involves either $–NH_3^+$ or $–NH_2^+$ group, hence protonated N-atom; this applies to both tautomers of mono and di-protonated forms.
2) When more than one intramolecular NH--N contact is formed then H-atoms of both protonated groups are always involved.
3) In general, the largest number of the intramolecular NH--N short contacts, typically three, is found in the LECs for both tautomers of mono and di-protonated forms.
4) The size of an intramolecular ring formed by the NH--N contacts appears to be of significance and most stable conformers form largest possible rings.
5) The latter trend does not apply to conformers with two terminal groups being protonated; only 5m-IRs are formed and, typically, three consecutive such rings are present among the LECs.
6) When a single terminal group is protonated, then the largest possible, 11m-MR is preferentially formed. This feature is observed among ten **HL_p** and three **H_2L_{ps}** LECs.
7) When a single –NH–group is protonated, then largest possible 8m-IR is preferentially formed; this is observed among top six lowest energy **HL_s** conformers.
8) It appears that large rings contribute in stabilizing manner to molecular energy more than smaller rings. We found significant differentiation in relative energies of **HL_p**, **HL_s** and **H_2L_{ps}** conformers for which small sets of LECs, all with either 11m- or 8m-rings, are observed. Note that all the **H_2L_{pp}** conformers form only 5m-IRs and we observe (i) many of them within a relatively small energy window and (ii) typically, most stable conformers form more rings.

3.3 Topological preferences of LAPs

Molecular graphs were generated for all 480 final structures obtained from Stage 4 of the CSP, *i.e.*, 30 **HL_s**, **HL_p**, **H_2L_{sp}** and **H_2L_{pp}** conformers optimized at all four levels of theories were analysed. Unfortunately, direct comparison of topological properties was not a straightforward process because often different number of atomic interaction lines (AILs), with associated critical points, CPs, was observed for the same conformer optimized at different LoT. An example is shown in Fig. 5 where four and five dashed lines representing intramolecular AILs

are observed for the C_p01 conformer optimized at B3LYP and MP2, respectively; one short CH--HC contact at B3LYP is not linked by an AIL.

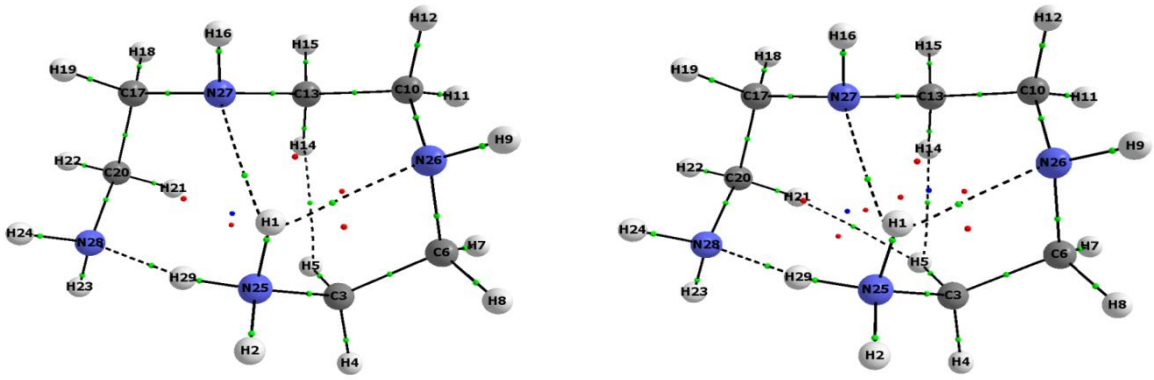

(a) (b)

Fig. 5 Molecular graphs of the C_p01 conformer showing different sets of AILs due to different levels of theory these structures were optimized at: (a) – B3LYP and (b) – MP2

Furthermore, it is important to stress that AILs are observed for most (but not all) of the short intramolecular NH--N contacts identified from the geometrical analysis of conformer. Because of that, we based our comparative approach on contacts linked by AILs at MP2.

For each molecular graph generated at MP2, a dedicated table was prepared showing atoms involved in a particular interaction, interatomic distance and electron density at a CP, ρ_{CP}, as well as short contacts without an AIL – an example for C_p02, the LEC found at MP2, is shown in Table 1 which is supplemented (for convenience) by a molecular graph shown in Fig. 6. A similar approach was adopted for the top 15 conformers of **HL_p**, **HL_s**, **H_2L_{ps}** and **H_2L_{pp}** and relevant data is provided in Tables S3–S6 of the SI.

Table 1 Interatomic distance and electron density at a CP of interactions found on molecular graph, shown in Fig. 4, of C_p02 (the LEC at MP2) together with a short contact which is not linked by AIL

	Atoms		**d(A,B)**	**ρ_{CP}**
Interaction	**A**	**B**	**Å**	**a.u.**
NH•••N	N28	H2	1.750	0.0507
	N26	H1	2.040	0.0287
CH•••N	N27	H4	2.601	0.0115
CH•••HC	H4	H15	2.124	0.0105
N•••N	N25	N27	2.897	0.0147
Contact without AIL				
NH--N	N27	H1	2.478	–

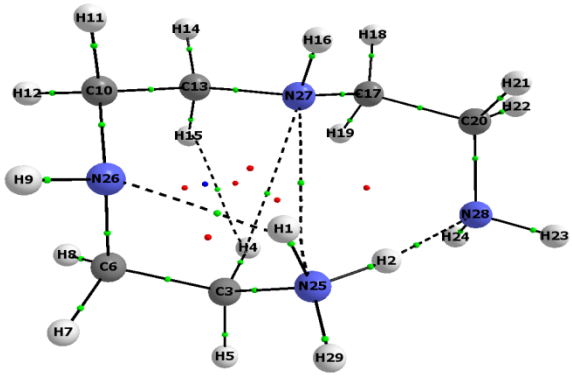

Fig. 6 A molecular graph of C_p02, the lowest energy conformer obtained at MP2

From the analysis of data presented in Tables S3–S6 of the SI, it became clear that the appearance of AIL is not governed by the interatomic distance. For instance, (i) one observes an AIL in C_p04 with d(N,H) = 2.512 Å, but there is no AIL in C_p02, C_p05, C_p06 or C_s06 where shorter d(N,H) = 2.478, 2.482, 2.473 and 2.365 Å are observed, respectively, (ii) there is only one AIL observed even though two NH--N contacts have the same d(N,H) = 2.559 Å - see $C_{pp}10$ in Table S6 of the SI where N29 and H24 are linked by AIL but N29 and H8 are not, and finally (iii) atoms separated by larger distance might be linked with AIL, *e.g.*, for $C_{pp}12$ shown in Table S6 of the SI, an AIL is observed for N29 and H24 with d(N,H) = 2.566 Å but no AIL is observed for N29 and H8 with d(N,H) = 2.511 Å. Moreover, there are numerous additional AILs (with small ellipticity) linking atoms one would not expect; we refer here to CH•••HC intramolecular interactions which, surprisingly, are mainly present in the LECs of the monoprotonated forms but, even more unexpectedly, are not observed at all in the ten highest in energy conformers of **HL** tautomers. Considering $\mathbf{H_2L}$ tautomers, these CH•••HC interactions were completely absent in the conformers of the $\mathbf{H_2L_{ps}}$ tautomer and only were found in four highest in energy conformers of the $\mathbf{H_2L_{pp}}$ tautomer. Furthermore, some conformers of the **HL** tautomers might be considered as topologically 'unstable' (even though no negative frequencies are present, hence energetically they are stable) because unusual atoms are linked with highly bent AILs, *e.g.*, we observe the CH•••N (in C_s03 shown in Table S4 of the SI), N•••N (in C_p02) or CH•••C (in C_p04) interactions which are shown in Table S3 of the SI.

It is now well established that the ρ_{CP} *vs.* d(A,B) should follow an exponential relationship when the same kind of interaction in very much similar molecular environment takes place. A good example one can find in [31] where a large number of intramolecular H-bonds was examined in a numerous conformers of pamidronate (bisphosphonate). Clearly, one might expect that the NH•••N interactions in both tautomers of **HL** should fully meet this requirement and we have decided to test whether topological 'anomalies' (this also includes appearance of AILs representing CH•••HC) have some influence on ρ_{CP} *vs.* d(N,H) relationships involving

'legitimate' interactions, classically regarded as the intra-molecular H-bonds. We noted that the NH•••N interactions, *e.g.*, in MP2-generated **HL$_p$** conformers, could be grouped in terms of interatomic distances. We found fifteen short contacts with d(N,H) = 1.70±0.03 Å for which ρ_{CP}(H•••N) = 0.058±0.05 a.u., eight medium length contacts, d(N,H) = 2.04±0.08 Å with ρ_{CP}(H•••N) = 0.029±0.04 a.u. and five longer contacts, d(N,H) = 2.47±0.09 Å with ρ_{CP}(H•••N) = 0.014±0.02 a.u. and they all follow an excellent ρ_{CP} *vs*. d(N,H) relationship - see Fig. 7a for **HL$_p$** conformers where, as it should be, an exponential decay in ρ_{CP}(NH•••N) is observed with an increase in the interatomic distance regardless on the presence of additional AILs or whether a structure could be regarded as topologically stable or not. Considering the **HL$_s$** conformers, the NH•••N interactions are characterised by overall longer interatomic distances; they are dominated by eighteen medium d(N,H) of 2.11±0.05 Å with ρ_{CP}(H•••N) = 0.025±0.03 a.u. rather than short range contacts; we found only eight shorter contacts with d(N,H) = 1.74±0.05 Å and ρ_{CP}(H•••N) = 0.054±0.05 a.u. We have decided to combine the data related to all the NH•••N

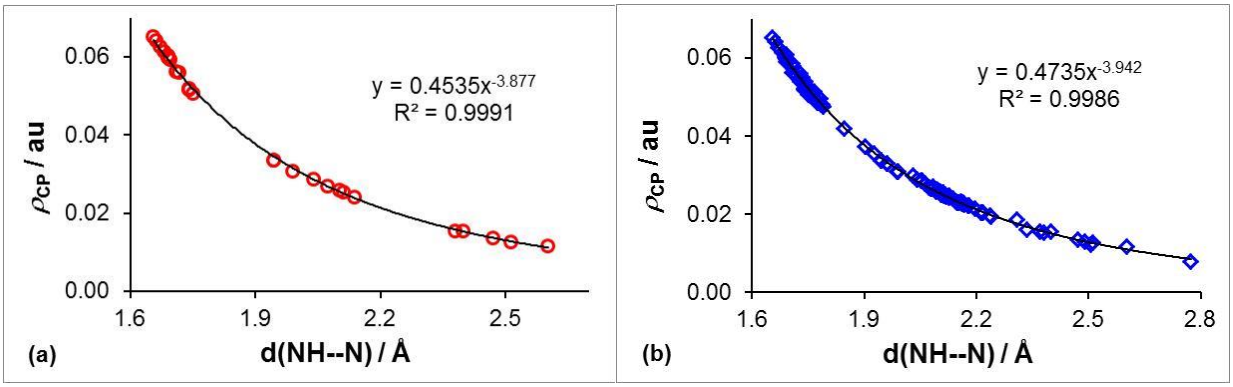

Fig. 7 Exponential decrease in ρ_{CP} with interatomic distance d(N,H) for all NH•••N interactions in 15 LECs for: part a –HL$_p$ at MP2, part b – HL$_p$ and HL$_s$ at MP2 and B3LYP combined

interactions in 15 lowest energy conformers of both, **HL$_p$** and **HL$_s$**, tautomers and generated the ρ_{CP} *vs*. d(N,H) relationship; it was pleasing to note that the trend and quality of the resultant relationship was as seen in Fig. 7a; as an example, a relationship obtained at B3LYP is shown in Fig. S6 in the SI. Finally, we combined all the relevant data obtained at MP2 and best performing B3LYP and, as seen in Fig. 7b, this had no influence on the quality of the relationship. This observation can also be used in support of our recommendation related to the use of B3LYP. The trend seen in Fig. 7b shows that the overall density distribution between atoms does not depend to a large extent on the level of theory used even though (i) the electronic energies of the same conformers and (ii) interatomic distances between the same atoms involved in the NH--N contacts differ significantly at the MP2 and B3LYP level of theory. One might rationalize this observation in terms of the same underlying physical fundamentals, namely the

Ehrenfest and Feynman forces. The interplay between potential and kinetic energy densities appears to be such that density distribution at critical points throughout the molecules varies exponentially with the interatomic distance; note that the combined ρ_{CP}(H•••N) data comes from **HL$_s$** and **HL$_p$** tautomers which are characterized by the same kind and a number of atoms, hence the same molecular environment is present in both tautomers. Similar quality relationships were found for the NH•••N interactions also in **H$_2$L** tautomers which are characterized by dominance of medium d(N,H) values; forty d(N,H) = 2.11±0.04 Å and thirty d(N,H) = 2.12±0.08 Å in the **H$_2$L$_{pp}$** and **H$_2$L$_{ps}$** tautomers, respectively.

According to QTAIM, the 'glue' that binds atoms together is the shared electron density at critical point, ρ_{CP}, and this can be used as a measure of relative strength of an interaction. Focusing on the leading and by far strongest NH•••N intramolecular interactions, it appears that, on average, they are weaker in **HL$_s$** than in **HL$_p$** when measured by the individual values of ρ_{CP}. Also, the stronger the interaction (the larger ρ_{CP}) the more significant stabilizing energy contribution to a molecular system is expected. Because there are several NH•••N interactions in the LECs and assuming that these stabilizations are additive, it is reasonable to evaluate their combined contribution [32], denoted here as $\rho_{CP}(H\bullet\bullet\bullet N)_{total}$, which represents summed densities at CPs of these interactions within a conformer. From preliminary inspection of topological data we found, just as an example, that the lowest energy conformers of **HL$_p$** (C_p02) and **HL$_s$** (C_s04) have only two NH•••N interactions and the $\rho_{CP}(H\bullet\bullet\bullet N)_{total}$ value of 0.079 a.u. in C_p02 is larger than that in C_s04 (0.074 a.u.); however, the electronic (*E*) and Gibbs free (*G*) energies of C_s04 are more negative (C_s04 is more stable than C_p02). In contrast, the $\rho_{CP}(H\bullet\bullet\bullet N)_{total}$ value obtained for C_{ps}01 (0.073 a.u.) is larger than that found in C_{pp}12 (0.049 a.u.) and this corresponds to their relative stability; the values of *E* and *G* of C_{ps}01 are ~4 and 2 kcal/mol, respectively, lower (more negative) than that of C_{pp}12.

To gain better assessment and understanding, we initially plotted the sum of ρ_{CP} values for all NH•••N interactions linked with AIL in each conformer against its relative energy for the fifteen lowest in energy conformers of each tautomer optimised at MP2. The best such relationship was obtained for **HL$_s$** which is shown in Fig. 8a – points marked with asterisks follow a reasonable trend with R^2 = 0.936 (dashed line); an example of rather poor relevant trend (R^2 = 0.496) is shown for **HL$_p$** as asterisks in Fig. 8b. Thereafter we plotted the sum of ρ_{CP} values for all AIL-linked NH•••N and CH•••HC interactions found for each conformer against their relative energy – see circles in Fig. 8. This resulted in significantly worse trend (R^2 = 0.804, solid line) for **HL$_s$** but somewhat better trend (R^2 = 0.511, dotted line) in case of **HL$_p$** in Fig. 8b. Finally, we have decided to sum up densities at all CPs within a conformer, regardless whether AIL could be

regarded as representing acceptable for a chemist an intramolecular interaction – an example of much improved relationship, with $R^2 = 0.733$, is shown as triangles in Fig. 8b.

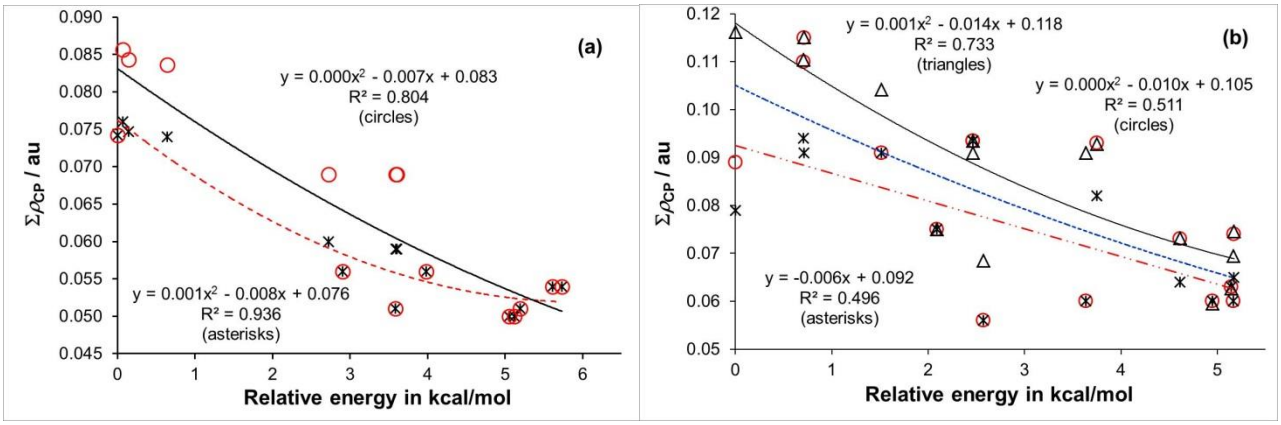

Fig. 8 Relationship between $\Sigma\rho_{CP}$ and relative energy of top 15 conformers of (a) HL_s and (b) HL_p. Asterisks represent the NH•••N interactions; circles stand for sum of the NH•••N and the CH•••HC interaction, and triangles (in b) are used for the sum of all interactions linked by AILs in a conformer

At first glance the overall picture obtained from these relationships appears to be inconsistent and highly confusing. However, one must recall that (i) the appearance of an AIL (or a bond path) was interpreted as a privileged exchange-correlation channel, hence it does not have to be present between all short geometrical contacts and (ii) it is well-known that an increase in electron density in the bonding interatomic region always results in a stabilizing energy contribution made by an intramolecular interaction [33]. An analysis of Tables S3-S6 in the SI provides further explanation. Namely, there are numerous conformers with either NH--N and/or CH--HC contacts (some shorter than those linked by AIL) which are not linked with AILs, hence it was impossible to include their contributions in the relationships drawn in Fig. 8. Moreover, the best trend obtained for **HL_p** includes, besides NH•••N and CH•••HC, also CH•••N and N•••N interactions when linked by AILs and this significantly improved the regression coefficient, from $R^2 = 0.496$ to 0.733. All the above leads to the conclusion that it is most likely impossible to generate high quality $\Sigma\rho_{CP}$ *vs.* ΔE relationships in the case of large(r) molecules with densely packed atoms. Perhaps, one would need input from all interatomic areas characterized by non-uniform density distribution, a characteristic feature of QTAIM- as well as NCI-defined critical points, to improve such relationship.

3.4 Insight from an NCI analysis

From the above analyses it follows that the stability of *trien* conformers depends mainly on the strength and number of the NH•••N interactions present. It is also clear that the (de)stabilizing role of the CH•••HC interactions in the LECs of *trien* (or more generally, in LAPs) cannot be

neglected. Furthermore, since the ρ_{CP} value of an interaction does not necessarily give sufficient information as to the stabilizing or otherwise nature of an interaction [34-37], we therefore decided to gain further insight from the recently developed non covalent interaction index (NCI) technique [38]. This is also because the presence of other intramolecular interactions, which are invisible to the QTAIM technique but must contribute to (de)stability of a conformer, can be uncovered by the NCI method.

NCI is not widely used yet, hence to facilitate interpretation of NCI-generated data, it is in order to give a brief outline of NCI descriptors used to describe a nature and kind of interaction. This technique is making use of the real space visualization and interpretation of the electron density (ρ) and its reduced gradient $s(\rho)$ to locate regions of space where the electronic density distribution deviates from homogeneity due to the formation of a non-covalent inter- or intramolecular interaction [39]. Using the sign of the second eigenvalue (λ_2) of the Hessian matrix, NCI analysis is used to classify interactions as (de)stabilizing according to the topology (decrease/increase) of electron density distribution. Conveniently, results obtained from the NCI analysis are displayed using either 2D or 3D plots. The 2D plot shows variation in the reduced density gradient as a function of the electron density oriented by the sign of its λ_2. Within this plot, the presence of an intramolecular interaction is shown by the appearance of a spike/trough in regions of low electron density. To visualize the interactions, 3D isosurfaces are generated which reveal the spatial location of inter or intramolecular interactions and their nature within a molecular system [38, 39]. In order to rank interactions according to their strength and nature, a colouring scheme is utilized. According to this scheme: (i) stabilizing interactions – also referred to as type I NCI interactions characterized by density increase in the interatomic region – are coloured in blue, (ii) destabilizing – NCI type II – interactions are coloured in red, indicative of density depletion, and (iii) van der Waals – NCI type III – delocalized weak interactions are shown in green. The colour intensity corresponds to the strength of an interaction, *i.e.*, greater intensity refers to stronger interaction and *vice-versa*. The shape of the isosurfaces of the three main NCI-types interactions can also vary, *e.g.*, (i) small, flat, pill-shaped isosurface for stabilizing interaction has been attributed to its bi-centric nature, (ii) red cigar-shaped isosurface (elongated along directions of decreasing density within an intramolecular ring) was linked with destabilizing interaction, and (iii) sheet-like extended surfaces were interpreted as weak van der Waals interactions. In the case of flexible molecules, such as amino acids and aliphatic polyamines, the formation of non-covalent interactions often leads to steric crowding and intramolecular rings. A closure of a ring, an interatomic region between interacting atoms, typically appears as a bicoloured almond-shaped NCI isosurface in a 3D NCI plot with one end being coloured in green-to-blue (this represents a stabilizing contribution) and the other

end is usually red which indicates multi-centric repulsion amongst atoms involved in ring formation. All the above are generally used and accepted NCI descriptor and we will attempt to utilize them in the interpretation of intramolecular interactions.

Selected examples of the NCI 3D plots for each tautomer are shown in Fig. 9 and relevant plots for top five lowest energy conformers of each tautomer are shown as Figs. S7-S10 in the SI. Let us first focus on the strongest, NH•••N, interactions:

a) All large rings, 11m-MR and 9m-IR, are characterized by a dark blue pill-shaped NCI isosurface which corresponds very well to highly stabilizing contribution recovered by QTAIM in the form of AILs with relatively large ρ_{CP} values. Furthermore, these dark blue discs are not surrounded by red rings; this indicates that there is no strain in this interatomic region and this agrees well with general notion related to this type of interaction.

b) Without an exemption, the formation of all 5m-IRs with AILs is recovered by the presence of an almond-shaped bicoloured NCI isosurface. The blue region, as it should, coincides with the presence of an interaction critical point and the red region is due to the steric crowding (caused by an intramolecular ring formation) and it points at the area where a ring critical point (point of lowest density within a ring) is identified from a QTAIM analysis.

c) The NCI analysis also revealed the presence of additional NH•••N interactions which were not recovered from the QTAIM-based analysis – a typical example is seen for C_s05 in Fig. 9 where a bluish colour of the NCI plot is observed between N29 and H17 (similar is found *e.g.*, for the contact between N27 and H29 in $C_{ps}03$ in Fig. S9 in the SI). These AIL-absent NH•••N interactions which form intramolecular 5-membered rings also resulted in almond-shaped bicoloured NCI isosurfaces (as found for AIL-linked 5-membered rings) but their isosurfaces have less intense colours which is indicative of being weaker interaction.

We change our focus on few and rather unexpected interactions now:

a) There is a N27--N25 contact in the MP2 lowest energy C_p02 conformer which is linked by an AIL, hence it might be represented as N27•••N25. Classically, such an interaction would be seen as repulsive and a cause of intramolecular strain, hence destabilizing a molecule. It is then most interesting to note that indeed, as one would expect due to the presence of AIL, a blue isosurface is observed between these two N-atoms but, most surprisingly, it is not surrounded by red-coloured area. The blue in the centre and red on the outskirts discs are synonymous with strain caused by crowded atomic environment and have been reported for, *e.g.*, water dimer where d(O,H) of intermolecular interaction was smaller than that at the equilibrium [40] or for water dimer with forced-to-be O-atoms in close proximity [34].

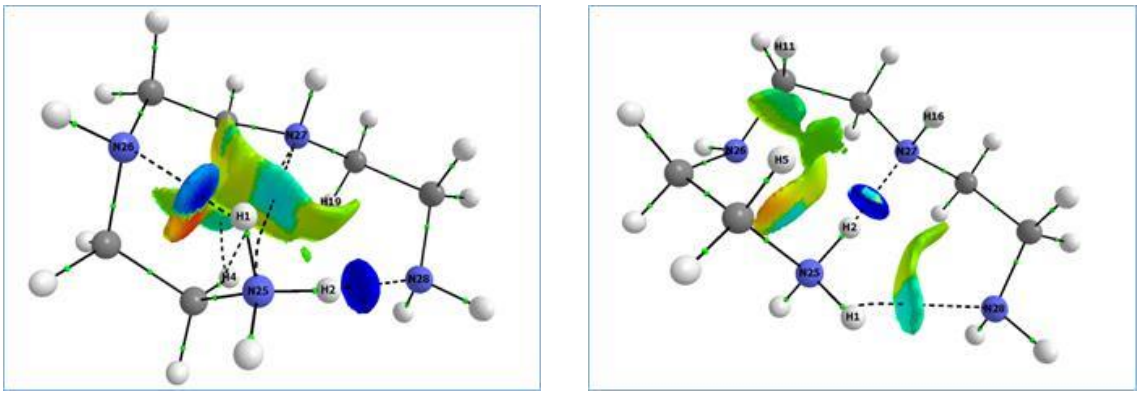

C_p02 C_p05

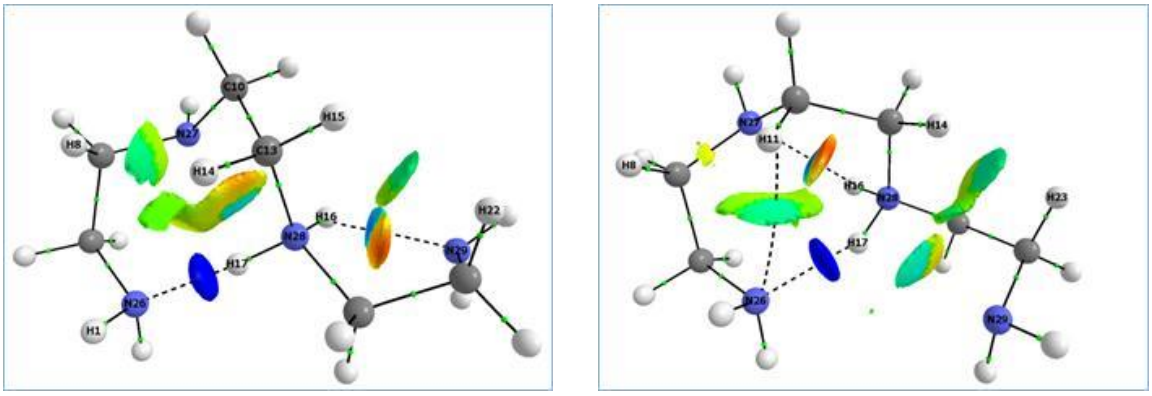

C_s04 C_s05

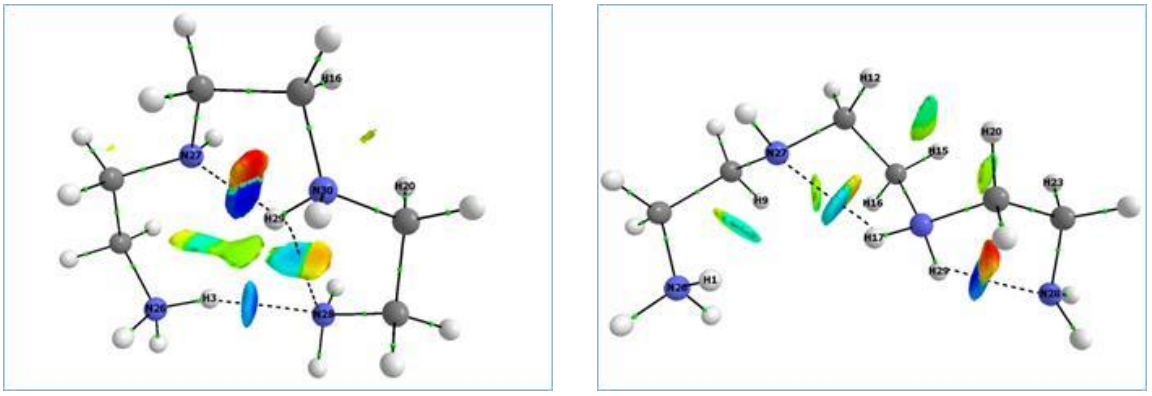

$C_{ps}01$ $C_{ps}14$

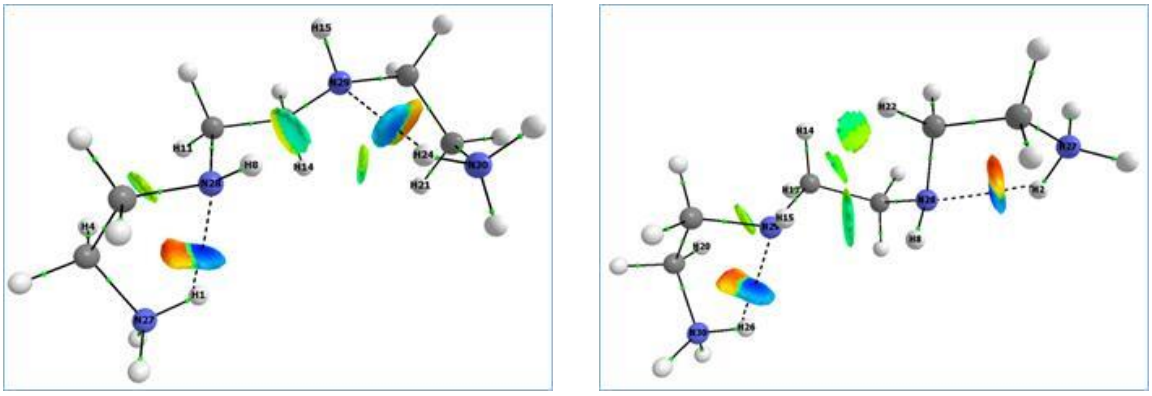

$C_{pp}12$ $C_{pp}11$

Fig. 9 NCI isosurfaces (RDG isovalue = 0.5 a.u.) for selected conformers of (a) HL_p, (b) HL_s, (c) H_2L_{ps} and (d) H_2L_{pp}. Isosurfaces are coloured from blue to red using a $-0.03 \leq \rho(r) \times \text{sign}(\lambda_2) \leq +0.03$ range

(a) Another example of unusual interaction is seen in Cs05 (Fig. 9) where the AIL-linked CH11•••N26 interaction is observed; also in this case no trace of intramolecular strain is recovered by the NCI-defined isosurface and, in general, we observe very much the same features as described in details for the N27•••N25 interaction in C_p02.

Considering the CH•••HC interactions identified by NCI technique, we note that:

(a) None of them appears to be strained; notice that all relevant isosurfaces, within a bonding region of the interactions, are not coloured in red.
(b) Some of interatomic H--H regions display isosurfaces coloured in blue (which might be interpreted as being of significantly stabilizing nature, *e.g.*, CH14•••H20C in C_{ps}14 in Fig. 9 or CH14•••H20C in C_{ps}14 in Fig. S9 in the SI.
(c) Interestingly, these blue (or light-blue) interatomic regions are parts of almond-shaped bicoloured NCI isosurfaces and, importantly, the other colour is not red (or reddish) which strongly suggests that the resultant 5-memebred rings are not strained either. What one observes, instead, is the change from blue to a mixture of yellow and green colours, a transition from stabilizing (increased density) to van der Waals – NCI type III - delocalized weak interaction.
(d) In many instances, the number of the CH•••HC interactions identified by NCI technique is larger when compared with QTAIM, *e.g.*, two QTAIM- and three NCI-identified interactions in C_p01 or none QTAIM- and three NCI-identified interactions in C_{ps}14. However, the NCI isosurfaces are virtually indistinguishable for both, AIL-linked and AIL-absent, interactions and also compare well with weaker NH•••N interactions without AILs.

Finally, we would like to focus on intramolecular regions in conformers where large rings are formed. There is a striking difference between intramolecular regions of the 11m-MRs and 8m-IRs. One observes large multi-coloured NCI isosurfaces which represent multi-centric interactions and are (i) predominantly blue-to-yellow-to-green in the case of 11m-MRs (typically in C_p conformers) whereas (ii) a significant degree of red colouring is present in the case of the 8m-IRs as seen, *e.g.*, in C_s conformers. When this observation is combined with isosurfaces obtained for 5m-IRs, it appears that the intramolecular strain increases with a decrease in the size of a ring and this correlates well with earlier observation where we found that the most stable conformers form 11m-MR and largest possible intramolecular rings. The fact that NCI managed to recover some degree of intramolecular strain within 8m- and 5m-IRs, which are formed by some of the NH--N contacts, provides additional credibility to our interpretation of the CH--HC contacts as strain free.

We have not performed the NCI analysis on all conformers (hundreds of them) because (i) this is simply not feasible and (ii) this methodology is not perfectly suited for quantitative analysis. Instead, we focused on the lower energy conformers where numerous CH--HC and some other unusual contacts were found and, understandably, uncovering their nature was of paramount importance. The NCI results showed that indeed (i) there are many additional and not negligible intramolecular interactions which, if quantified, might better explain the relative stabilities (energies) of LECs found here, and (ii) the presence of the CH--HC contacts in the LECs has not resulted in the increase of these conformers' energies and most likely, at least in some cases, it might have resulted in additional stabilizing contributions. One must stress, however, that this does not mean that some of CH--HC are indeed destabilizing a molecule and clearly one would have to perform an in depth examination of each case to fully uncover their nature, but this is not the theme of this work. Moreover, from NCI isosurfaces one can gain an insight on localized to two-atom fragment nature of an interaction as well as the presence of intramolecular strain can be deduced, but this tells us nothing about an energy contribution made by such interaction to the entire molecular system.

There is another important observation to be made. As shown in Fig. 8(b), an improved trend was obtained when all AIL-linked interactions were accounted for and this correlates well with the above interpretations of the 3D NCI plots. It is possible, as mentioned above, that inclusion of all remaining interactions (which are not linked by AIL) might improve such trend even further. We are of an opinion, however, that this will not result in an excellent relationship (ΔE *vs.* ρ_{CP}) which could be used as a reliable predictive tool because (i) the density at critical points is not a direct measure of the strength of an interaction; similar ρ_{CP} for different kind of interactions might represent different energy contributions, (ii) very much the same density can be observed for attractive and repulsive interactions, and (iii) one still has to account for intramolecular strain but this is not possible at present. On the positive note, although the quantitative interpretation of relative stability of conformers, not only LAPs, appears to be just a dream, one can gain an invaluable insight on qualitative interpretation using geometric and topological descriptors and features which, as demonstrated in this work, can identify definite lower and definite higher in energy conformers. It is reasonable to assume that findings of this work should be useful also in the analysis of conformers in the gas phase; relevant work is in progress to verify this assumption and we hope to report on this soon.

3.5 Theoretical prediction of protonation sequence

As we have stressed in the introduction, our main focus is to predict theoretically the first protonation site of polyamines because of the 'contradicting' interpretations of experimental

results reported to date. It appears, however, that most recent papers, particularly those involving cluster expansion analysis (CEA) of NMR data, (i) are consistent in that a mixture of primary and secondary tautomers is always proposed but (ii) report significantly different %-fractions for each tautomer, $\mathbf{HL_p}$ and $\mathbf{HL_s}$. For instance, considering well-studied tetramine spermine, 30% ($\mathbf{HL_p}$) and 70% ($\mathbf{HL_s}$) was reported by Borkovec at al [8] whereas essentially equal molar ratio for both tautomers was found by Albelda et al [41], both results came from CEA. This is not entirely surprising when one recalls that the cluster expansion analysis (i) involves a lot of unknowns to be fitted into experimental data (*e.g.*, there are 16 parameters in the case of tetramine spermine [42]) and (ii) the protonation microconstant of each protonation site must be determined from the NMR studies (often experimental NMR protonation constants differ significantly from those determined by most accurate technique, glass electrode potentiometry [43]) and, hence this unavoidably carries some degree of mathematical/statistical and experimental uncertainty.

Furthermore, theoretical studies [12], which were based on linear triamines, predicted a tautomer with secondary N-atom to be the only **HL** form present and, interestingly, we found the same when linear conformers of *trien* were used. It was then of utmost interest and importance to find out whether this prediction will still hold when lowest energy conformers of $\mathbf{HL_p}$ and $\mathbf{HL_s}$, those with %-fraction above 5, were used. It was pleasing to note that a mixture of about 40 to 60% of $\mathbf{HL_p}$ and $\mathbf{HL_s}$, respectively, was obtained in an implicit water environment. This correlates well with recent experimental/theoretical models and clearly indicates an importance of using LEC of each tautomer. Also, one must realize that the obtained 40:60 ratio must not be taken literally as it must depend on a solvation model as well as level of theory used (we found *e.g.*, 1% and 54% of $\mathbf{HL_p}$ from modelling at HF and B97D level of theory, respectively) and, unfortunately, there is no easy way to *rigorously* verify any theoretical model experimentally. In support of this, Weisell et al [44] found, from QM-modelling of pentamine 1,12-diamino-3,6,9-triazadodecane (SpmTrien) involving explicit water molecules, that 91% ($\mathbf{HL_p}$) and 9% ($\mathbf{HL_s}$) is formed with short chain being protonated preferentially (66% short and 25% long chain for the $\mathbf{HL_p}$ form) which clearly contradicts all earlier as well recent studies whereas from the CEA of NMR data they obtained 94% ($\mathbf{HL_p}$) and 6% ($\mathbf{HL_s}$) with long chain, as expected, being protonated preferentially, ~84%. Moreover, note that their findings, in general, are not in agreement with other studies as they predicted a very small fraction of $\mathbf{HL_s}$ whereas this tautomer was found to be significant in many polyamines and even dominating, *e.g.*, in spermine [5, 8, 41].

On the other hand, one can argue that experimentally or theoretically predicted variation (within reasonable limits) in the %-fraction of these two tautomers, $\mathbf{HL_p}$ and $\mathbf{HL_s}$, should not

have any significance in real, *e.g.*, biological environment; from that perspective most important founding is that indeed these two tautomeric forms can easily change from one form to another implying that each is available to suite a specific biological process best.

Finally, few comments on the **H_2L** form. It has been stressed [42] that two protons must be separated by the minimum of four $–CH_2-$ groups with one proton being located on the terminal nitrogen. From our conformational search it follows that the lowest energy conformers of **H_2L** are characterized by a large number of structures with two terminal 5m-IRs involving protonated either primary or secondary N-atom (the difference in their energy being negligible). Because the lowest energy conformers of **H_2L_{ps}** are characterized by the presence of the largest possible 11m-MR (a feature found also for most stable **HL** conformers), they are also predicted to dominate a mixture of the two, **H_2L_{ps}** and **H_2L_{pp}**, tautomers. Although this does not correlate very well with the cluster expansion analysis of NMR data [8] (it predicts **H_2L_{pp}** to constitute 76% of deprotonated forms of *trien*) one must note that (i) the presence of **H_2L_{pp}** was predicted here whereas this is not the case at all when linear structures are used, (ii) formation of **H_2L_{ps}** does meet the requirement of minimum separation by the –CH2- groups, and (iii) it is well known that a proton exchange is among fastest reactions known and it is quite possible that conformers with terminal 5m-IRs can easily exchange a proton between the primary and secondary N-atom. Furthermore, in the case of spermine, **H_2L_{ps}** was found to be either a dominant tautomer with 67 %-fraction [8] or making only 40% contribution to the population [41]; interestingly, in both cases data came from the same, CEA protocol and this exemplifies again significant degree of uncertainty in NMR-generated experimental data and their interpretation by CEA.

It has been suggested from the analysis of 13C-NMR studies [42] that terminal N-atoms are protonated first because their better disposition for solvation with the aqueous solvent. To test this, explicit water molecules in computational modelling must be used. Even though this must be seen as extremely time-demanding modelling, we decided to embark on this project because (i) we can make use of an effective conformational search protocol developed and tested here as well as (ii) data generated at the B3LYP level were found here to be sufficient for the purpose of the study (the same level of theory was also used recently in modelling of SpmTrien [44].

3.6 Relative performance of levels of theory

3.6.1.Comparative structural analysis

Two main types of intramolecular short contacts, NH--N and CH--HC, were identified in the various conformers. Classically, the CH--HC contact is interpreted as a steric clash destabilizing a molecule but, surprisingly, it was present in many low energy conformers. Although the van der Waals atomic radii values given by Bondi (1.20Å and 1.55 Å for H- and N-atoms, respectively) are the most widely accepted and cited in chemical literature, subsequent investigations [45-47], based on crystallography and electron density topology, have argued that they were overestimated for certain atoms, among them hydrogen. Consequently it is possible that some of the CH--HC contacts identified here might be due to this overestimation.

We have shown here that the general structural features of each group of conformers is determined by their intramolecular contacts, hence we compared the distances of all NH--N and CH--HC short contacts in the MP2 structures to those of relevant structures obtained at HF, B3LYP and B97D. The absolute value of each deviation from the distance at MP2, $|\Delta d(A,B)|$, was then used to calculate average distance deviation (and its standard deviation) for each conformer. Full data sets for the two types of short contacts identified in LECs of **HL** and $\mathbf{H_2L}$ tautomers are presented in Tables S7-S14 of the SI and, as an example, see Table 2. The comparative geometrical analysis of all NH--N contacts in conformers of the **HL** and $\mathbf{H_2L}$ tautomers leads to the following observations and trends:

- Relative to MP2, the best estimates of d(N,H) were obtained at B3LYP; we found the following trend, HF > B97D > B3LYP, for the $\left|\Delta d(N,H)\right|$ values.
- HF consistently overestimates d(N,H) and, on average, the $\left|\Delta d(N,H)\right|$ value of ~0.22 Å is an order of magnitude larger when compared with data obtained at B3LYP for all conformers of **HL** and $\mathbf{H_2L}$.
- Although, in most cases, B3LYP also overestimates d(N,H), it consistently generates the averaged $\left|\Delta d(N,H)\right|$ of ~0.02 Å which, in turn, is about halve of what we obtained at B97D.
- B97D consistently shows somewhat larger number of underestimated diatomic distances, particularly in the case of $\mathbf{HL_p}$ conformers.

Focusing now on analysis of $\Delta d(H,H)$, we found the following:

- HF was unable to reproduce the MP2-generated CH--HC contacts in many cases, particularly in the $\mathbf{H_2L_{pp}}$ conformers.
- Generally, the magnitude of deviation from the MP2 values for d(H,H) follows the HF > B3LYP > B97D trend.

- Both, HF and B3LYP, overestimate d(H,H) values, but B97D shows an almost equal number of positive and negative deviations.

Table 2 Relative to MP2 values of d(N,H), performance of HF, B3LYP and B97D in terms of Δd(N,H) obtained for top LECs of HL_p (all values in Å)

Conformer	**Contact**	**d(N,H)**	**Δd_{HF}**	**Δd_{B3LYP}**	**Δd_{B97D}**
C_p03	N28--H29	1.741	0.214	0.029	–0.060
	N26--H2	2.136	0.136	0.032	0.107
	N27--H2	2.379	0.138	–0.044	–0.131
C_p02	N28--H2	1.750	0.219	0.025	–0.072
	N26--H1	2.040	0.127	0.038	0.081
	N27--H1	2.478	0.066	0.025	–0.001
C_p01	N28--H29	1.740	0.227	0.016	–0.079
	N26--H1	2.073	0.125	0.036	0.086
	N27--H1	2.398	0.052	–0.029	–0.043
C_p05	N27--H2	1.680	0.276	0.031	–0.061
	N28--H1	2.470	0.303	0.020	–0.050
	N26--H2	2.482	0.053	0.050	0.078
	N28--H2	2.646	0.008	0.038	0.033
C_p04	N28--H2	1.740	0.242	0.032	–0.072
	N26--H29	2.101	0.162	0.012	0.077
	N27--H29	2.512	0.157	–0.005	–0.031
C_p09	N27--H2	1.689	0.245	0.001	–0.061
	N28--H1	1.989	0.563	0.003	–0.140
C_p08	N27--H1	1.717	0.315	0.036	–0.083
C_p06	N27--H29	1.691	0.286	0.043	–0.018
	N28--H2	1.944	0.914	0.016	–0.124
	Overall Average for |Δd|:		**0.220**	**0.023**	**0.065**
	Overall StDev for |Δd|:		**0.183**	**0.014**	**0.032**
	Overall Average for Δd:		***0.220***	***0.019***	***0.006***
	Overall StDev for Δd:		***0.183***	***0.019***	***0.073***
	Combined data for HL_p and HL_s				
	Overall Average for |Δd|:		**0.220**	**0.036**	**0.082**
	Overall StDev for |Δd|:		**0.159**	**0.020**	**0.040**
	Overall Average for Δd:		***0.216***	***0.032***	***0.009***
	Overall StDev for Δd:		***0.164***	***0.026***	***0.092***

In summary, (i) B3LYP performs significantly better in reproducing an overall geometry of the lowest in energy conformers than B97D; this is because B3LYP is better in predicting the strongest interactions, NH•••N, which play a decisive role in determining the LAPs structures, (ii) HF is not suitable for a rigorous analysis as it performed much inferior when compared with B3LYP or B97D, and (iii) if analysis of the CH--HC contacts was the main focus of an investigation then, not surprisingly, one should use B97D rather than B3LYP.

3.6.2 Comparative topological analysis

As an example, the computed differences, *e.g.*, at HF, $\Delta\rho_{CP}^{HF} = \rho_{CP}^{HF} - \rho_{CP}^{MP2}$, for a number of LECs of **HL$_p$** are shown in Table 4 where, in addition, the ρ_{CP} values obtained at MP2 as well as the combined data for both, **HL$_p$** and **HL$_s$**, tautomers are also included. The full data sets for both tautomers of **HL** and **H$_2$L** are presented in Table S15-S21 in the SI.

The analysis of all $\Delta\rho_{CP}^{LoT}$ values, obtained for the NH•••N interactions, reveals that:

- A lot of interactions observed at MP2 were not recovered at HF, *e.g.*, only 1 among 16 was found in the case of C_{pp} conformers.
- All MP2 NH•••N interactions were reproduced at B3LYP but few are missing at B97D.
- The magnitude of deviation from MP2 values, $\Delta\rho_{CP}^{LoT}$, generally follows the $\Delta\rho_{CP}^{HF} > \Delta\rho_{CP}^{B97D} > \Delta\rho_{CP}^{B3LYP}$ trend.
- On average, HF significantly underestimates the values of ρ_{CP} (they differ already at the second decimal place of a.u. when compared with those obtained at MP2) whereas B97D generates somewhat overestimated data, particularly in the case of **HL$_p$** (typically on third decimal place of au).
- The best performing B3LYP reproduced the MP2 ρ_{BCP} values well, typically, average absolute difference, avr($|\Delta\rho_{CP}^{B3LYP}|$), is characterized by low numbers on the third decimal place of a.u., *e.g.*, 0.0017±0.0014 and 0.0030±0.0019 a.u. was found for **HL$_p$** and **HL$_s$**, respectively. For comparison, at B97D we obtained avr($|\Delta\rho_{CP}^{B97D}|$) of 0.0074±0.0049 and 0.0066±0.0038 a.u. for **HL$_p$** and **HL$_s$**, respectively.

Similar analysis was performed for the CH•••HC interactions – see data displayed in Tables S19-S20 in the SI. The most significant difference, when compared with trends found for the NH•••N interactions, is the fact (as one would expect) that the MP2 ρ_{CP} values were best reproduced at B97D and we found the following trend, $\Delta\rho_{CP}^{HF} > \Delta\rho_{CP}^{B3LYP} > \Delta\rho_{CP}^{B97D}$.

It is important to note that results of our comparative geometrical and topological analysis are in agreement. Therefore, we recommend B3LYP as the optimum level of theory among those we have examined for reproducing MP2 geometries and topological properties of low energy conformers of LAPs. Our recommendation is strengthened by the finding that the NH•••N interaction, which is most dominant, hence determines the structure adopted by conformers, is best reproduced at B3LYP.

Table 3 Relative to MP2 ρ_{CP} values, performance of HF, B3LYP and B97D in terms of $\Delta\rho_{CP}$ for NH•••N interactions in top LECs of HL_p (all values in a.u.). In addition, the combined data for HL_p and HL_s is provided

Conformer	**Interaction**	ρ_{CP}	$\Delta\rho_{CP}^{HF}$	$\Delta\rho_{CP}^{B3LYP}$	$\Delta\rho_{CP}^{B97D}$
C_p03	N28•••H29	0.0517	–0.0215	–0.0025	0.0102
	N26•••H2	0.0241	–0.0057	–0.0016	–0.0047
	N27•••H2	0.0153	–0.0040	0.0007	0.0036
C_p02	N28•••H2	0.0507	–0.0213	–0.0021	0.0115
	N26•••H1	0.0287	–0.0071	–0.0022	–0.0043
C_p01	N28•••H29	0.0521	–0.0224	–0.0010	0.0128
	N26•••H1	0.0269	–0.0064	–0.0019	–0.0042
	N27•••H1	0.0154	–0.0025	0.0000	0.0005
C_p05	N27•••H2	0.0614	–0.0305	–0.0035	0.0118
	N28•••H1	0.0136	–	–0.0007	0.0008
C_p04	N28•••H2	0.0518	–0.0234	–0.0028	0.0120
	N26•••H29	0.0258	–0.0070	–0.0008	–0.0037
	N27•••H29	0.0126	–	–0.0005	0.0000
C_p09	N27•••H2	0.0601	–0.0278	0.0007	0.0115
	N28•••H1	0.0308	–0.0197	0.0001	0.0117
C_p08	N27•••H1	0.0559	0.0238	–0.0037	0.0143
C_p06	N27•••H29	0.0599	–0.0305	–0.0050	0.0046
	N28•••H2	0.0336	–	–0.0007	0.0117
	Overall Average($\lvert\delta\rho_{CP}\rvert$):		**0.0169**	**0.0017**	**0.0074**
	Overall StDev($\lvert\delta\rho_{CP}\rvert$):		**0.0102**	**0.0014**	**0.0049**
	Overall Average($\delta\rho_{CP}$):		***–0.0137***	***–0.0015***	***0.0056***
	Overall StDev($\delta\rho_{CP}$):		***0.0144***	***0.0016***	***0.0070***
	Combined data for HL_p and HL_s				
	Overall Average($\lvert\delta\rho_{CP}\rvert$):		**0.0151**	**0.0023**	**0.0063**
	Overall StDev($\lvert\delta\rho_{CP}\rvert$):		**0.0097**	**0.0015**	**0.0040**
	Overall Average($\delta\rho_{CP}$):		***–0.0088***	***–0.0008***	***0.0037***
	Overall StDev($\delta\rho_{CP}$):		***0.0158***	***0.0027***	***0.0066***

4. Conclusions

From an in depth analysis (involving structural, QTAIM and NCI properties) of hundreds of conformers of **HL** and **H_2L** *trien* tautomers, a combined (MM/DFT) conformational search protocol (CSP) was developed to generate representative sets of lowest energy conformers (LECs) of linear aliphatic polyamines (LAPs) in reasonable time. For the purpose of this study, sets of lowest, medium and higher energy conformers were investigated at HF, B3LYP, B97D and MP2 levels of theory with an aim of finding out structural and topological preferences in implicit aqueous environment.

Considering structural preferences, we found common numerous trends for both, mono- and di-protonated tautomers, such as (i) when a single NH--N short contact is formed (this is characteristic for higher energy conformers) then it always involves either $–NH_3^+$ or $–NH_2^+$ group, hence the protonated N-atom, (ii) when more than one intramolecular NH--N contact is observed then H-atoms of both protonated groups are always involved, (iii) LECs are characterized by largest possible number of the intramolecular NH--N short contacts and most stable conformers form largest possible rings. Furthermore, (i) when a single terminal group is protonated, then the largest possible, 11m-MR is preferentially formed. This feature is observed among ten $\mathbf{HL_p}$ and three $\mathbf{H_2L_{ps}}$ LECs, (ii) when a single –NH–group is protonated, then largest possible 8m-IR is preferentially formed; this is observed among top six lowest energy $\mathbf{HL_s}$ conformers and (iii) with two terminal groups being protonated; only 5m-IRs are formed and, typically, three consecutive such rings are present among the LECs (all N-atoms in a molecule are involved). Finally, results obtained showed that large rings contribute in stabilizing manner to molecular energy more than smaller rings. We found significant differentiation in relative energies of $\mathbf{HL_p}$, $\mathbf{HL_s}$ and $\mathbf{H_2L_{ps}}$ conformers for which small sets of LECs, all with either 11m- or 8m-rings, are observed; the $\mathbf{H_2L_{pp}}$ conformers form only 5m-IRs and the more rings the more stable conformer is formed.

QTAIM-based topological analysis revealed the presence of many atomic interaction lines (AILs), in LECs in particular, which in most cases could be seen as 'legitimate' or an orthodox bond path. In general, most but not all NH--N short contacts were linked by AILs; in some instances contacts with longer d(N,H) were linked by AIL even though a shorter contact was present. Excellent relationships between ρ_{CP} and d(N,H) were found for all tautomers but, more importantly, combined data sets from B3LYP and MP2 also resulted in near perfect exponential relationships for each tautomer. Quite unexpectedly, we found numerous AILs linking CH--HC intramolecular contacts; they were present mainly in the LECs of the mono-protonated forms but, even more unexpectedly, they were absent in the ten highest in energy conformers of **HL** tautomers. On the other hand, these CH•••HC interactions were completely absent in the conformers of the $\mathbf{H_2L_{ps}}$ tautomer and only were found in four highest in energy conformers of the $\mathbf{H_2L_{pp}}$ tautomer. To gain further insight, we used NCI technique. It revealed the presence of many additional intramolecular NH--N as well as CH--HC interactions. 3D NCI-defined isosurfaces showed that there is no qualitative difference between AIL-linked and AIL-absent contacts of the same kind, NH--N or CH--HC. Also, following classical interpretation, NCI isosurfaces revealed an increase in an intramolecular strain with a decrease in the size of a ring formed by the NH--N; 11m_MR appeared to be strain free whereas 5m-IR showed significant degree of strain. Surprisingly, in all cases of 5m-IR formed by the CH--HC interaction, no strain

was observed. It is rather difficult to rationalize significance of QTAIM-defined AILs and NCI-defined isosurfaces in the interatomic region of the CH--HC contacts in terms of their (de)stabilizing energy contribution to a molecular system as these two phenomena simply represent a localized density increase between atoms involved; hence, we embarked on an extensive and dedicated for the purpose separate studies to explain fully the chemical nature and energy contribution made by these and some other totally unexpected contacts discovered mainly in the lowest energy conformers. One might add to this that an attempt to correlate summed density values at critical point against relative energy of conformers failed to generate good quality relationships (regardless whether only the strongest NH•••N or combined, NH•••N plus CH•••HC, interactions were accounted for).

Significance and usefulness of the developed conformational search was confirmed here as we were able to predict (i) a mixture of $\mathbf{HL_p}$ and $\mathbf{HL_s}$ conformers in accord with experimental data reported recently [5]; formation of $\mathbf{HL_s}$ as the only form was predicted when linear conformers were used, and (ii) a possibility of presence of both $\mathbf{H_2L}$ tautomers was also recovered, although a significantly different relative %-fractions were obtained here when compared with cluster expansion analysis of NMR data [8]; using linear conformers, formation of $\mathbf{H_2L_{ps}}$ was predicted as the only species formed. Clearly, this work strongly supports the view that conformational search must be seen as a prerequisite for theoretical studies of molecules characterized by almost an infinite conformational freedom, such as LAPs.

Finally, from the extensive analysis of all the data obtained at different levels of theory it became clear that (i) B3LYP was best reproducing MP2 data; it can be reliably used for this type of investigations and only few (typically 3 to 5) LECs could (should) be optimized and analysed at MP2, and (ii) HF should rather be avoided as it has not performed well neither in the search of LECs nor was able to recover topological properties.

Acknowledgement

This work is based on the research supported in part by the National Research Foundation of South Africa (Grant Numbers 87777) and the University of Pretoria.

Compliance with Ethical Standards

This work fully complies with Ethical Standards. An informed consent was reached to publish this work.

Conflict of Interest

The authors declare that they have no conflict of interest.

References

1. Agostinelli E, Marques MPM, Calheiros R, Gil FPSC, Tempera G, Viceconte N, Battaglia V, Grancara S, Toninello A (2010) Polyamines: fundamental characters in chemistry and biology. Amino Acids 38:393–403.
2. Bachrach U (2010) The early history of polyamine research. Plant Phys Biochem 48:490–495.
3. Batista de Carvalho LAE, Marques MPM, Tomkinson J (2006) Transverse Acoustic modes of biogenic and α,ω-polyamines: a study by inelastic neutron scattering and Raman spectroscopies coupled to DFT calculations. J Phys Chem A 110:12947–12954
4. Paoletti P, Ciampolini M, Vacca A (1963) Thermochemical studies VII. Heats and entropies of stepwise Neutralization of Piperazine and trien. J Phys Chem 67:1065–1067.
5. Hague DN, Moreton AD (1994) Protonation Sequence of Linear Aliphatic Polyamines by ^{13}C NMR Spectroscopy. J Chem Soc Perkin Trans 2:265–270.
6. Dagnall SP, Hague DN, McAdam ME (1984) ^{13}C Nuclear Magnetic Resonance Study of the Protonation Sequence of some Linear Aliphatic Polyamines. J Chem Soc Perkin Trans 2:1111–1114.
7. Delfini M, Segre AL, Conti F, Barbucci R, Barone V, Ferruti P (1980) On the Mechanism of Protonation of Triamines. J Chem Soc Perkin Trans 2:900–903.
8. Borkovec M, Cakara D, Koper GJM (2012) Resolution of Microscopic Protonation Enthalpies of Polyprotic molecules by means of cluster expansions. J Phys Chem B 116:4300–4309.
9. Hedwig GR, Powell HKJ (1973) Thermodynamics of Complex Formation of 1,5,8,12-Tetra-azadodecane with Copper(II) Ions and Protons in Aqueous Solution. J.C.S. Dalton 793–797.
10. Barbucci R, Fabbrizzi L, Paoletti P (1972) Thermodynamics of complex formation of Aliphatic Linear Tetra-amines. ΔH and ΔS for the Reactions of 1,5,9,13- Tetra-azatridecane with Protons and Some Bivalent Transition-metal Ions. J.C.S. Dalton 745–749.
11. Kimberly MM, Goldstein JH (1981) Determination of pKa Values and Total Proton Distribution Pattern of Spermidine by Carbon-13 Nuclear Magnetic Resonance Titrations. Anal Chem 53:789–793
12. Cukrowski I, Matta CF (2011) Protonation sequence of linear aliphatic polyamines from intramolecular atomic energies and charges. Comput Theoret Chem 966:213–219.
13. Marques MPM, Batista de Carvalho LAE (2007) Vibrational spectroscopy studies on linear polyamines. Biochem Soc Trans 35:374–380.

14. Govender KK, Cukrowski I (2009) Density Functional Theory in Prediction of Four Stepwise Protonation Constants for Nitrilotripropanoic Acid (NTPA). J Phys Chem A 113:3639–3647.
15. Govender KK, Cukrowski I (2010) Density Functional Theory and Isodesmic Reaction Based Prediction of Four Stepwise Protonation Constants, as log KH(n), for Nitrilotriacetic Acid. The Importance of a Kind and Protonated Form of a Reference Molecule Used. J Phys Chem A 114:1868–1878.
16. Reyzer ML, Brodbelt JS (1998) Gas-phase Basicities of Polyamines. J. Am. Soc. Mass Spectrom 9:1043–1048.
17. Ilioudis CA, Hancock KSB, Georganopoulou DG, Steed JW (2000) Insights into supramolecular design from analysis of halide coordination geometry in a protonated polyamine matrix. New J Chem 24:787–798.
18. Batista de Carvalho LAE, Laurenc LE, Marques MPM (1999) Conformational study of 1,2-diaminoethane by combined ab initio MO calculations and Raman spectroscopy. J Mol Struc-Theochem 482-483:639–646.
19. Carballeira L, Mosquera RA, Rios MA (1988) Conformational analysis of polyfunctional aminic compounds by molecular mechanics: Part 1. Methanediamines and 1,3-diazacyclohexanes. J Mol Struc-Theochem 176:89–105.
20. Carballeira L, Mosquera RA, Rios MA, Tovar CA (1988) Conformational analysis of polyfunctional amino compounds by molecular mechanics. : Part II. 1,2-Ethanediamine, 1,3-propanediamine and 1,4-diazacyclohexanes. J Mol Struc-Theochem 193:263–277.
21. Frisch MJ, Trucks GW, Schlegel HB et al (2009) Gaussian 09, Revision D.1, Gaussian, Inc., Wallingford CT.
22. Tomasi J, Persico M (1994) Molecular interactions in Solution: An overview of Methods Based on Continuous distribution of the Solvent. Chem Rev 94:2027–2094.
23. Miertusˇ S, Scrocco E, Tomasi J (1981) Electrostatic interaction of a solute with a continuum. A direct utilization of AB initio molecular potentials for the prevision of solvent effects. Chem Phys 55:117–129.
24. Cammi R, Tomasi J (1995) Remarks on the use of the apparent surface charges (ASC) methods in solvation problems: Iterative versus matrix-inversion procedures and the renormalization of the apparent charges. J Comput Chem 16:1449–1458.
25. Wilke JJ, Lind MC, Schaefer HF, Csaszar AG, Allen WD (2009) Conformers of Gaseous Cysteine. J Chem Theory Comput 5:1511–1523

26. Sanchez-Lozano M, Cabaleiro-Lago EM, Hermida-Ramon JM, Estevez CM (2013) A Computational study of the protonation of simple amines in water clusters. Phys Chem Chem Phys 15: 18204–18216.
27. Bader RFW (1990) Atoms in Molecules: A Quantum Theory. Oxford University Press, Oxford, UK
28. Keith TA (2013) AIMALL (Version 13.11.04), TK Gristmill Software, Overland Parks KS, USA, <aim.tkgristmill.com>
29. Contreras-García J, Johnson ER, Keinan S, Chaudret R, Piquemal JP, Beratan D, Yang WJ (2011) NCIPLOT: a program for plotting noncovalent interaction regions. J Chem Theory Comput 7:625–632.
30. Spartan ’10 (2010) Wavefunction, Inc.: Irvine, CA.
31. Arabieh M, Karimi-Jafari MH, Ghannadi-Maragheh M (2013) Low-energy conformers of pamidronate and their intramolecular hydrogen bonds: a DFT and QTAIM study. J Mol Model 19:427–438
32. Gronert S, O’Hair RAJ (1995) *Ab initio* Studies of Amino Acid Conformations. 1. The conformers of Alanine, Serine and Cysteine. J Am Chem Soc 117:2071–2081.
33. Pendás AM, Francisco E, Blanco MA, Gatti C (2007) Bond paths as privileged exchange channels. Chem Eur J 13:9362–9371.
34. Cukrowski I, de Lange JH, Adeyinka AS, Mangondo P (2015) Evaluating common QTAIM and NCI interpretations of the electron density concentration through IQA interaction energies and 1D cross-sections of the electron and deformation density distributions, Comput Theoret Chem 1053:60–76
35. Haaland A, Shorokhov DJ, Tverdova NV (2004) Topological analysis of electron densities: is the presence of an atomic interaction line in an equilibrium geometry a sufficient condition for the existence of a chemical bond? Chem Eur J 10:4416–4421.
36. Jablonski MJ (2012) Energetic and geometrical evidence of nonbonding character of some intramolecular halogen···oxygen and other Y···Y interactions. J Phys Chem A 116:3753–3764.
37. Dem’yanov P, Polestshuk P (2012) A Bond Path and an Attractive Ehrenfest Force Do Not Necessarily Indicate Bonding Interactions: Case Study on M_2X_2 (M= Li, Na, K; X= H, OH, F, Cl). Chem Eur J 18:4982–4993.
38. Johnson ER, Keinan S, Mori-Sánchez P, Contreras-García J, Cohen AJ, Yang WJ (2010) Revealing Noncovalent Interactions. J. Am. Chem. Soc. 132:6498–6506.

39. Chaudret R, de Courcy B, Contreras-García J, Gloaguen E, Zehnacker-Rentien A, Mons M, Piquemal JP (2014) Unraveling non-covalent interactions within flexible biomolecules: from electron density topology to gas phase spectroscopy. Phys Chem Chem Phys 16:9876–9891.
40. Contreras-García J, Yang WJ (2011) Analysis of hydrogen-bond interaction potentials from the electron density: Integration of Non-covalent interaction regions. J Phys Chem A 115:12983–12990
41. Albelda MT, Frías JC, García-España E (2007) Proton Transfer Reactions. Encyclopedia of Supramolecular Chemistry. 1:1: 1–37.
42. Bencini A, Bianchi A, Garcia-España E, Micheloni M, Ramirez JA (1999) Proton coordination by polyamine compounds in aqueous solution. Coord Chem Rev 188:97–156.
43. Frassineti C, Ghelli S, Gans P, Sabatini A, Moruzzi MS, Vacca A (1995) Nuclear Magnetic Resonance as a Tool for Determining Protonation Constants of Natural Polyprotic Bases in Solution. Anal Biochem 231:374–382
44. Weisell J, Vepsäläinen J, Peräkylä M (2013) Tautomeric populations of the charged species of 1,12-diamino-3,6,9-triazadodecane (SpmTrien) studied with computer simulations and cluster expansions. J Phys Org Chem 26:360–366.
45. Bondi A (1964) van der Waals volumes and Radii. J Phys Chem 68:441–451.
46. Rowland RS, Taylor R (1996) Intermolecular Non bonded Contact Distances in Organic Crystal Structures: Comparison with Distances Expected from van der Waals Radii. J Phys Chem 100:7384–7391.
47. Klein RA (2006) Modified van der Waals atomic radii for hydrogen bonding based on electron density topology. Chem Phys Lett 425:128–133.